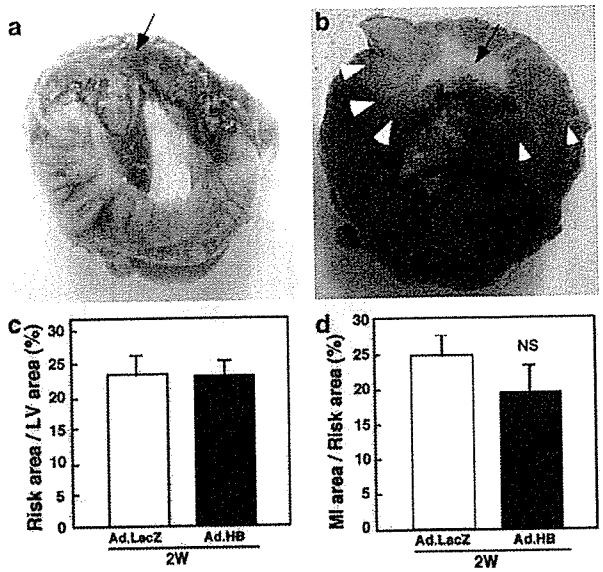

Figure 6 Macroscopic findings after adenoviral HB-EGF gene transduction in a rabbit MI model. (a) X-gal staining after Ad.LacZ injection into the border area. The arrow indicates the infarcted area. (b) Triphenyl tetrazolium chloride (TTC) and Evans blue staining define the risk areas (arrowheads), MI areas (arrow), and the intact (blue) areas. Graphs showing the risk area (c) and the MI area (d). Morphometric analysis of TTC/Evans blue-stained macroscopic slides 2 weeks after MI. NS: no significant difference.

not statistically significant (HB-EGF; 19.6±3.5% *vs* LacZ; 24.6±2.9%, $P=0.277$) (Figure 6d).

Cardiac Function and Histological Changes Following Adenoviral HB-EGF Gene Transduction in the Rabbit MI Model

Rabbits that received a control Ad.LacZ injection following MI clearly demonstrated a worsening of cardiac parameters such as left ventricular ejection fraction (LVEF) and left ventricular dimension at end-diastole (LVDd), as assessed by ultraechocardiography (UCG) at 2 and 4 weeks post-MI, compared with sham-operated rabbits that underwent neither adenoviral gene transduction nor MI (Figure 7a and b). Ad.HB-EGF injection after MI neither improved nor further worsened cardiac function, as assessed by LVEF or LVDd at 2 or 4 weeks compared with the Ad.LacZ-treated rabbits. On the other hand, anterior wall thickness (AWt) at 2 weeks (HB-EGF, 2.7±0.3 mm *vs* LacZ, 1.9±0.1 mm, $P<0.05$, Figure 7c) and the ratio of LV weight to body weight at 2 and 4 weeks were significantly increased by Ad.HB-EGF injection (2 weeks: HB-EGF, 1.59±0.06 *vs* LacZ, 1.44±0.03, $P<0.05$; 4 weeks: HB-EGF, 1.67±0.09 *vs* LacZ, 1.40±0.05, $P<0.05$) (Figure 7d); these findings were consistent with macroscopically observed hypertrophic changes (Figure 8). In addition, fibrosis in and around the MI area, which was induced by the MI itself, was increased by injection with Ad.HB-EGF at 2 and 4 weeks post-MI (2 weeks: HB-EGF, 7149±675 pixels *vs* LacZ, 4230±331 pixels, $P<0.001$; 4 weeks: HB-EGF, 6575±534 pixels *vs* LacZ, 4414±494 pixels, $P<0.05$) (Figure 8f).

Accordingly, histological examination revealed that individual cardiomyocytes at the border area were remarkably hypertrophic 2 and 4 weeks after Ad.HB-EGF injections (2 weeks: HB-EGF, 18.76±0.29 μm *vs* LacZ, 16.53±0.34 μm; $P<0.05$; 4 weeks: HB-EGF, 20.49±0.28 μm *vs* LacZ, 18.23±0.40 μm, $P<0.05$) (Figures 9 and 10). Thus, overexpression of HB-EGF markedly induces cardiomyocyte hypertrophy and fibrosis without affecting cardiac function, suggesting that this molecule plays an important role in accelerating the remodeling process after MI.

Characteristic Histological Findings in the MI Area

To clarify the mechanisms responsible for the enhancement of post-MI remodeling in the hearts treated with the HB-EGF gene during the subacute and chronic stages of MI, we performed histological examinations of rabbit hearts at 2 and 4 weeks post-MI. Increases in the number of cells in the MI area 2 and 4 weeks after MI were more prominent in rabbits receiving Ad.HB-EGF than in those receiving control Ad.LacZ (2 weeks: HB-EGF, 235±4 cells/field *vs* LacZ, 145±4 cells/field, $P<0.001$; 4 weeks: HB-EGF, 180±6 cells/field *vs* LacZ, 97±3 cells/field, $P<0.001$) (Figure 11a–c). Likewise, the number of proliferating (Ki-67 positive) cells increased more in the Ad.HB-EGF-treated rabbits than in those treated with Ad.LacZ (2 weeks: HB-EGF, 27.6±1.0 cells/field *vs* LacZ, 7.6±0.3 cells/field, $P<0.001$; 4 weeks: HB-EGF, 25.3±1.4 cells/field *vs* LacZ, 15.8±1.3 cells/field, $P<0.001$) (Figure 11d–f). Immunohistochemical studies demonstrated that these accumulated cells were primarily SMA-positive spindle myofibroblasts at both 2 and 4 weeks (2 weeks: HB-EGF, 62.7±0.8 cells/field *vs* LacZ, 38.0±0.9 cells/field, $P<0.001$; 4 weeks: HB-EGF, 48.6±1.7 cells/field *vs* LacZ, 22.7±1.1 cells/field, $P<0.001$) (Figure 11g–i), and RAM 11-positive macrophages at 2 weeks only (HB-EGF, 18.4±1.0 cells/field *vs* LacZ, 4.2±0.3 cells/field, $P<0.001$) (Figure 11j–l). On the other hand, the finding that more CD31-positive vascular endothelial cells were observed in the border area than in the remote area in both groups suggests an angiogenic effect induced by certain endogenous factors following MI (Figure 11m–o).

Interestingly, these vascular endothelial cells were not further increased by Ad.HB-EGF injections, in contrast to the significant increases observed in total cells, proliferating cells, myofibroblasts and macrophages, suggesting that HB-EGF most likely lacks angiogenic potential.

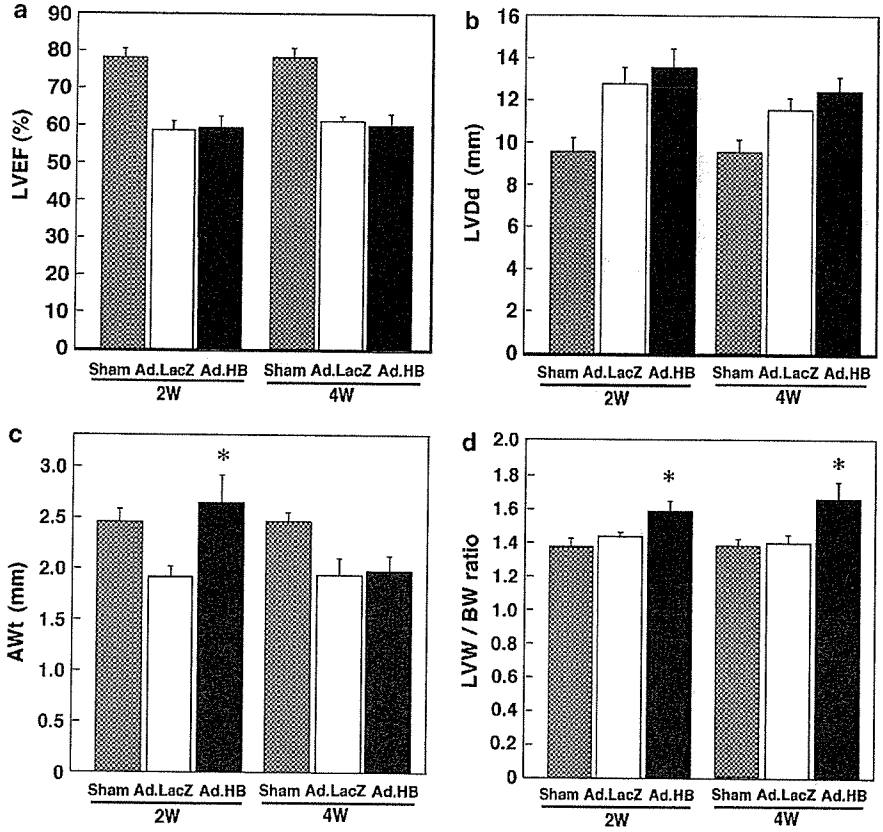

Figure 7 Echocardiographic measurements and left ventricular (LV) weight after adenoviral HB-EGF gene transduction in the postinfarct rabbit heart. Graphs showing the (**a**) LVEF, (**b**) LV size, (**c**) wall thickness, and (**d**) LV weight to body weight at 2 and 4 weeks after Ad.HB-EGF gene transduction in MI rabbits. Cardiac function parameters were assessed by echocardiographic examination. LVEF: left ventricular ejection fraction; LVDd: left ventricular dimension at end-diastole; AWt: anterior wall thickness; LVW: LV weight; BW: indicated body weight. 'Sham' indicates sham-operated rabbits without MI or adenoviral transduction. $^*P<0.05$.

Apoptosis in the MI Area after Adenoviral HB-EGF Gene Transduction

To estimate apoptosis in the MI area, TUNEL staining was performed. Unexpectedly, the number of TUNEL-positive cells was increased by Ad.HB-EGF injection at 2 weeks after MI (HB-EGF, $1.95\pm0.10\%$ *vs* LacZ, $1.04\pm0.09\%$, $P<0.001$) (Figure 12). Notably, most of the TUNEL-positive cells were costained with the anti-RAM11 antibody (Figure 13a and b), but not with anti-SMA antibody (Figure 13c), nor by markers for cardiomyocytes such as troponin I (Figure 13d). Moreover, TUNEL-positive signals were detected in the cytoplasm of some macrophages with intact nuclei. Thus, the TUNEL-positive cells may be not only apoptotic macrophages, but also viable macrophages that had phagocytosed other apoptotic cells (Figure 13b). Thus, *in vivo* HB-EGF gene transduction stimulated the activation of noncardiomyocytes, including macrophages, fibroblasts and myofibroblasts, but not endothelial cells, in and around the MI area, while at the same time inducing cardiac hypertrophy.

Discussion

This is the first study to explore directly the *in vivo* effects of overexpressed HB-EGF on heart remodeling after reperfused MI. In addition, our unique adenoviral gene transduction and overexpression approach allowed a preliminary assessment of the potential utility of HB-EGF in gene therapy. Overexpressed HB-EGF in the MI lesion did not result in a beneficial or therapeutic outcome, in contrast to results observed with HGF or IGF in rodent MI models, but rather exacerbated the remodeling process through the activation of specific types of noncardiomyocytes.

To identify the HB-EGF-related biological mechanism underlying heart failure, distinguishing the various phenotypic effects of HB-EGF from those of HGF and IGF may prove useful, because despite their differences all of these factors are essential cardiogenic growth factors as well as potent inducers of cardiac hypertrophy.[27,29,41] The most important difference between HB-EGF and HGF/IGF, which accounts for the observed discrepancy, is

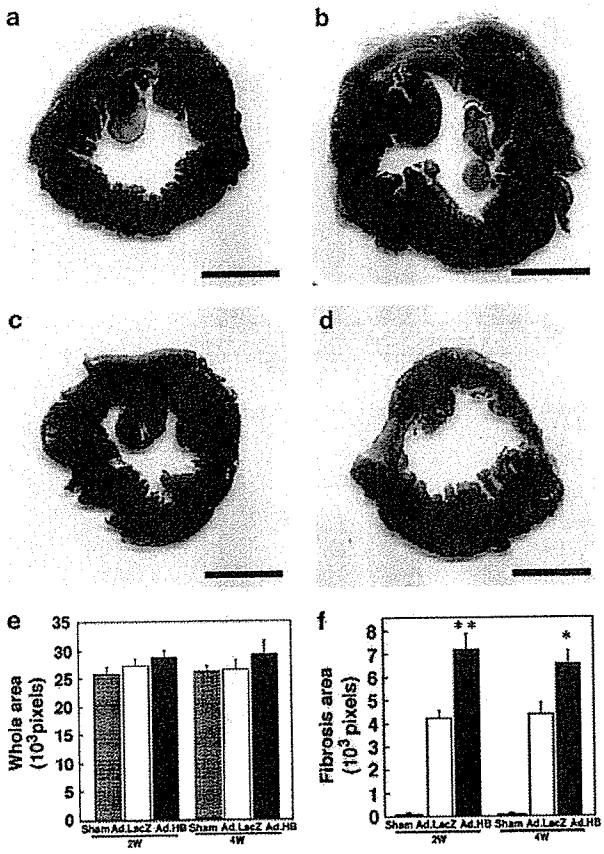

Figure 8 Macroscopic findings and histological analyses of transverse sections of hearts after adenoviral HB-EGF gene transduction. Fibrosis areas were stained blue with Masson's trichrome. (a) Ad.LacZ group (control) at 2 weeks after MI, (b) Ad.HB-EGF group at 2 weeks after MI, (c) Ad.LacZ group at 4 weeks after MI, (d) Ad.HB-EGF group at 4 weeks after MI. Graphs showing the whole areas (e) and fibrosis areas (f). The stained areas were morphometrically analyzed by counting pixels. Scale bar = 5 mm, $*P<0.05$, $**P<0.001$.

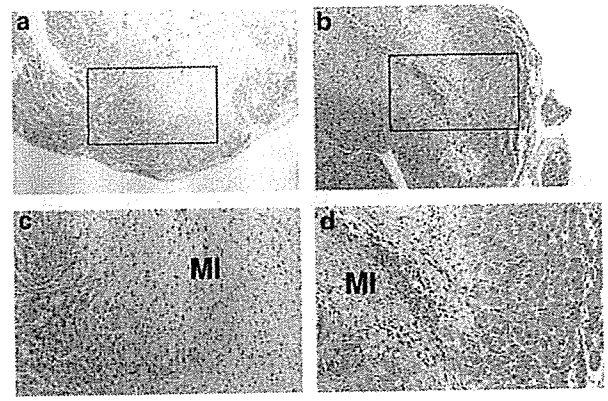

Figure 9 Histological findings at the MI border area after treatment. H–E-stained slides of LV 2 weeks post-MI. (a), (c) Ad.LacZ-treated rabbits and (b), (d) Ad.HB-EGF-treated rabbits. Squared-in areas in (a) and (b) (original magnification ×100) were magnified in (c) and (d) (original magnification ×400), respectively.

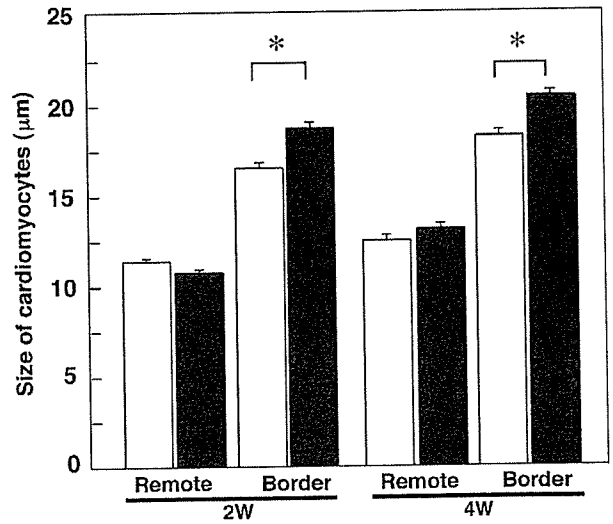

Figure 10 Size of cardiomyocytes at the remote and border areas of MI after treatment. The size of individual cardiomyocytes at the remote and border areas was morphometrically analyzed. $*P<0.001$.

the lack of a direct cytoprotective effect of HB-EGF on cardiomyocytes, in contrast to the potent cytoprotective effect observed for HGF and IGF in injured hearts.[27,29,41] This is a unique feature of HB-EGF, because most organogenic and/or organotrophic growth factors exert direct antiapoptotic effects, for example, HGF or IGF in mouse or rat cardiomyocytes[26–29] and HB-EGF in the small intestine.[42] In this regard, future studies to explore the differences among the molecules and signal transduction pathways involved in the activity of each growth factor would be biologically important.

Another important feature that differentiated HB-EGF from HGF and IGF was its observed lack of angiogenic activity. It should be noted that improvement of cardiac dysfunction after MI has been successfully achieved by gene therapy using angiogenic factors that do not directly act on cardiomyocytes.[29,43] This fact suggests that angiogenesis plays a crucial role in postinfarction remodeling, and that the absence of an angiogenic effect of overexpressed HB-EGF may be largely responsible for its lack of therapeutic action.

In addition, HB-EGF was revealed to have a mitogenic effect on fibroblasts, in contrast to the potent antifibrotic effect of HGF following MI.[27] Moreover, the characteristic finding after HB-EGF gene transduction was prominent accumulation of SMA-positive myofibroblasts and macrophages in the MI-affected areas. We previously reported that the infiltrating cells at the subacute stage post-MI

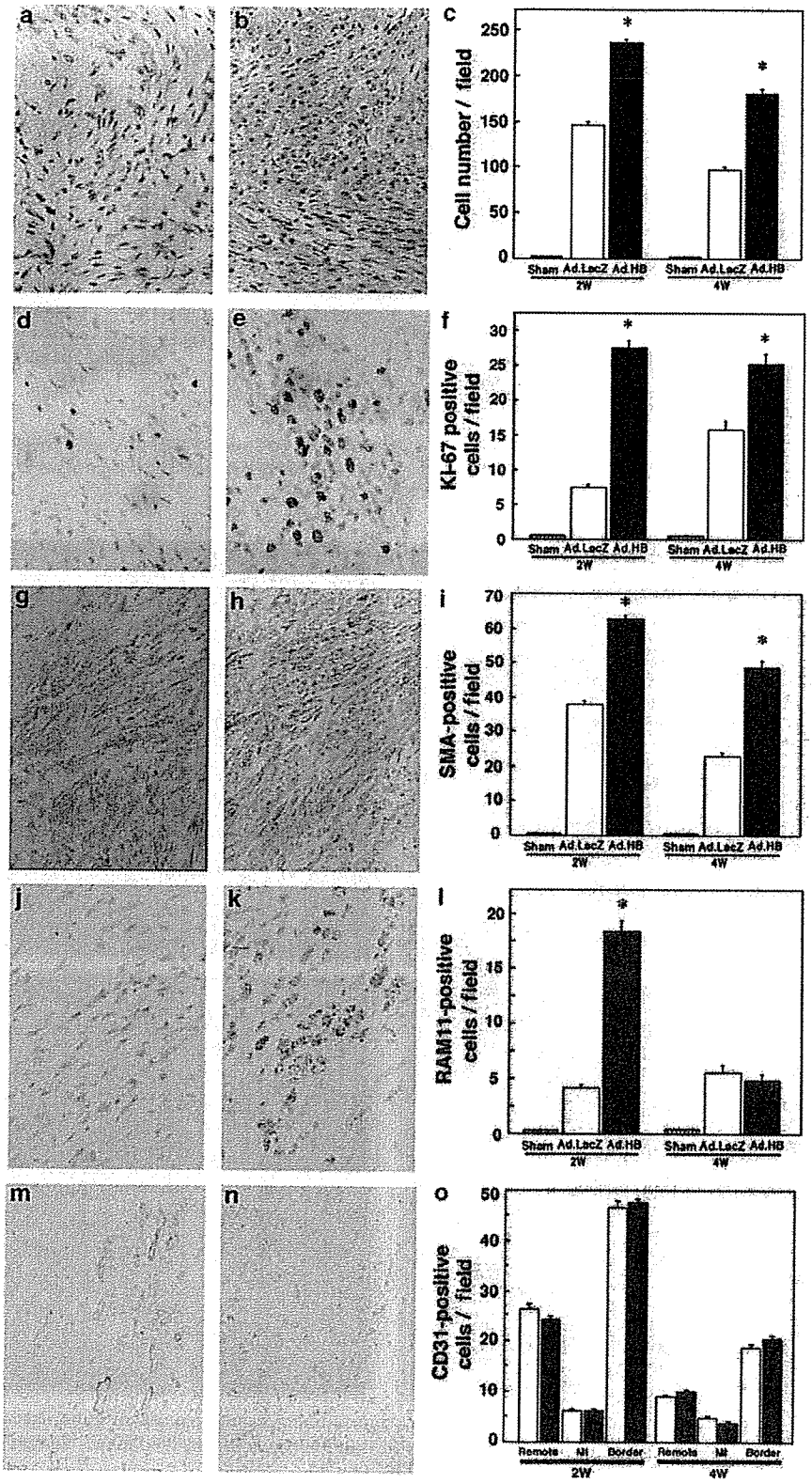

Figure 11 Histological and immunohistochemical findings in the MI area post-treatment. (**a**, **b**) H–E-stained-tissues, and immunohistochemically stained-tissues using (**d**, **e**) anti-Ki-67, (**g**, **h**) anti-SMA, (**j**, **k**) anti-RAM11, or (**m**, **n**) anti-CD31 antibodies 2 weeks after MI are shown (original magnification, × 400 for **a**, **b**, **d**, **e**, **g**, **h**, **j** and **k**, and × 100 for **m** and **n**). The number of positive cells in the field 2 and 4 weeks after MI were calculated and shown in the graphs (**c**, **f**, **i**, **l**, and **o**). *$P<0.001$.

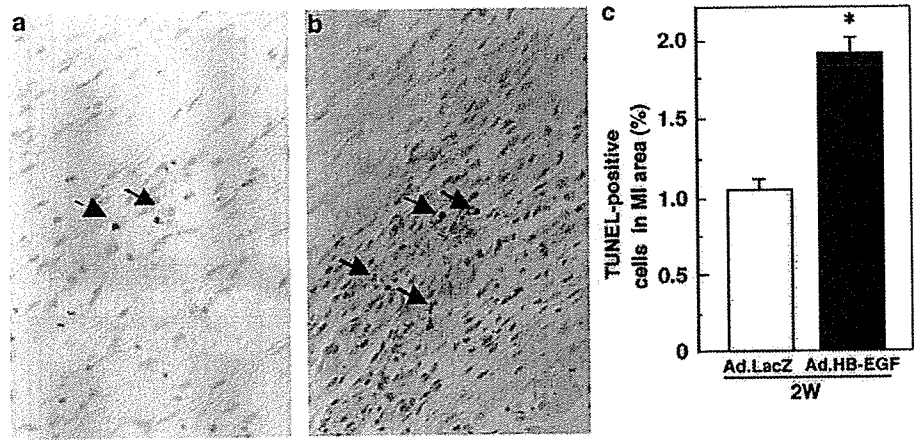

Figure 12 TUNEL staining in the MI area. TUNEL-positive cells (arrows) in the MI area 2 weeks after each treatment are shown. (**a**) and (**b**) indicate Ad.LacZ- and Ad.HB-EGF-treated rabbits, respectively. (**c**) The percentage of TUNEL-positive cells in the MI area was calculated by morphometric and quantitative analyses . $^*P<0.001$.

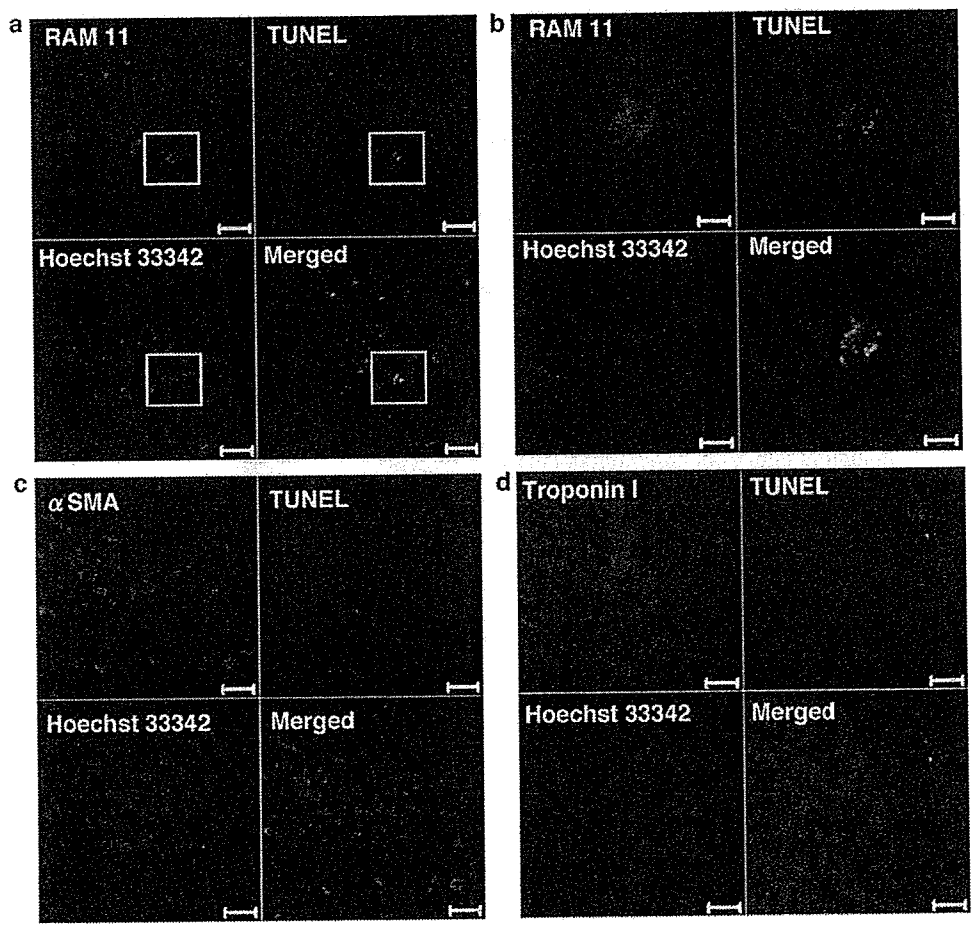

Figure 13 Immunofluorescent-TUNEL staining in the MI area. Laser confocal-microscopic analysis of slides that were triple-stained with TUNEL and (**a**, **b**) anti-RAM11, (**c**) anti-SMA and (**d**) anti-troponin I antibodies, and Hoechst 33342. Squared areas within (**a**) were magnified and shown in (**b**). Scale bars, 20 μm (**a**, **c**, **d**) and 5 μm (**b**).

were primarily macrophages, endothelial cells, and myofibroblasts, and that all of these cell types were entering apoptosis at an elevated rate.[37] Thus, the previously unknown factor that activates fibroblasts, myofibroblasts, and macrophages during post infarction remodeling is now strongly suggested to be

HB-EGF. Taken together with the lack of an agonistic death-inducible effect of HB-EGF directly on cardiomyocytes, pathologically upregulated HB-EGF may be responsible for activating these specific types of noncardiomyocytes, thus exacerbating post-MI remodeling.

The detailed molecular mechanisms by which HB-EGF activates these specific types of noncardiomyocytes remain to be elucidated. It was previously reported that HB-EGF stimulated the mitogenic and motogenic activities of smooth muscle cells,[4,7] and also that it reduced the expression of SMA in fibroblasts.[17] HB-EGF may play a regulatory role in the growth of fibroblasts and their transformation to myofibroblasts in the heart, as was suggested for the postinfarct kidney.[17] However, the biological relationship between HB-EGF and macrophages has yet to be studied, so future work to explore these molecular mechanisms would be interesting and fruitful. In this study, the overexpressed HB-EGF may consist not only of soluble HB-EGF, a potent mitogen for diverse cell types, but also membrane-bound proHB-EGF, whose functions may be diverse depending on cell types. In this context, future biological studies comparing the physiological and pathological effects of proHB-EGF on the heart with those of soluble HB-EGF may be of interest, although a suitable experimental system should be carefully established.

Finally, the recent finding that shedding of proHB-EGF resulted in cardiac hypertrophy suggests that upregulated HB-EGF might play a central role in hypertensive heart diseases.[24,25] However, overexpression of HGF and IGF induced cardiac hypertrophy, but inconsistently exhibited potent therapeutic and beneficial effects on the injured heart, including that damaged by MI.[27–29] Taken together with these facts, HB-EGF-induced cardiac hypertrophy may not be a sole or direct source of pathogenesis in MI, even though cardiac hypertrophy may, in fact, be involved in specific types of heart failure. In this context, the present results importantly imply that HB-EGF-induced exacerbation of remodeling may be a novel pathological mechanism for MI.

In conclusion, upregulated HB-EGF plays a pathological role in MI by activating specific types of noncardiomyocytes, leading to exacerbation of remodeling after MI. This novel fact may be useful for developing new therapeutics as well as for elucidating the mechanism of different types of heart failure, including MI.

Acknowledgements

This study was supported in part by Suzuken Memorial Foundation and a Grant-in-Aid for Scientific Research (C) from the Ministry of Education, Culture, Sports, Science and Technology of Japan. We thank Hatsue Oshika and Akiko Tsujimoto for their technical assistance.

References

1 Higashiyama S, Abraham JA, Miller J, *et al.* A heparin-binding growth factor secreted by macrophage-like cells that is related to EGF. Science 1991;251: 936–939.
2 Prenzel N, Zwick E, Daub H, *et al.* EGF receptor transactivation by G-protein-coupled receptors requires metalloproteinase cleavage of proHB-EGF. Nature 1999;402:884–888.
3 Ito N, Kawata S, Tamura S, *et al.* Heparin-binding EGF-like growth factor is a potent mitogen for rat hepatocytes. Biochem Biophys Res Commun 1994;198:25–31.
4 Higashiyama S, Abraham JA, Klagsbrun M. Heparin-binding EGF-like growth factor stimulation of smooth muscle cell migration: dependence on interactions with cell surface heparan sulfate. J Cell Biol 1993;122: 933–940.
5 Kiso S, Kawata S, Tamura S, *et al.* Liver regeneration in heparin-binding EGF-like growth factor transgenic mice after partial hepatectomy. Gastroenterology 2003; 124:701–707.
6 Iwamoto R, Mekada E. Heparin-binding EGF-like growth factor: a juxtacrine growth factor. Cytokine Growth Factor Rev 2000;11:335–344.
7 Miyagawa J, Higashiyama S, Kawata S, *et al.* Localization of heparin-binding EGF-like growth factor in the smooth muscle cells and macrophages of human atherosclerotic plaques. J Clin Invest 1995;95: 404–411.
8 Kalmes A, Daum G, Clowes AW. EGFR transactivation in the regulation of SMC function. Ann NY Acad Sci 2001;947:42–54; discussion 54–45.
9 Lemjabbar H, Basbaum C. Platelet-activating factor receptor and ADAM10 mediate responses to *Staphylococcus aureus* in epithelial cells. Nat Med 2002;8: 41–46.
10 Fu S, Bottoli I, Goller M, *et al.* Heparin-binding epidermal growth factor-like growth factor, a v-Jun target gene, induces oncogenic transformation. Proc Natl Acad Sci USA 1999;96:5716–5721.
11 Marikovsky M, Breuing K, Liu PY, *et al.* Appearance of heparin-binding EGF-like growth factor in wound fluid as a response to injury. Proc Natl Acad Sci USA 1993;90:3889–3893.
12 Tokumaru S, Higashiyama S, Endo T, *et al.* Ectodomain shedding of epidermal growth factor receptor ligands is required for keratinocyte migration in cutaneous wound healing. J Cell Biol 2000;151:209–220.
13 Nguyen HT, Bride SH, Badawy AB, *et al.* Heparin-binding EGF-like growth factor is up-regulated in the obstructed kidney in a cell- and region-specific manner and acts to inhibit apoptosis. Am J Pathol 2000;156:889–898.
14 Sakai M, Zhang M, Homma T, *et al.* Production of heparin binding epidermal growth factor-like growth factor in the early phase of regeneration after acute renal injury. Isolation and localization of bioactive molecules. J Clin Invest 1997;99:2128–2138.
15 Xia G, Rachfal AW, Martin AE, *et al.* Upregulation of endogenous heparin-binding EGF-like growth factor (HB-EGF) expression after intestinal ischemia/reperfusion injury. J Invest Surg 2003;16:57–63.
16 Pillai SB, Hinman CE, Luquette MH, *et al.* Heparin-binding epidermal growth factor-like growth factor protects rat intestine from ischemia/reperfusion injury. J Surg Res 1999;87:225–231.

17 Kirkland G, Paizis K, Wu LL, *et al.* Heparin-binding EGF-like growth factor mRNA is upregulated in the peri-infarct region of the remnant kidney model: *in vitro* evidence suggests a regulatory role in myofibroblast transformation. J Am Soc Nephrol 1998;9: 1464–1473.
18 Iwamoto R, Yamazaki S, Asakura M, *et al.* Heparin-binding EGF-like growth factor and ErbB signaling is essential for heart function. Proc Natl Acad Sci USA 2003;100:3221–3226.
19 Jackson LF, Qiu TH, Sunnarborg SW, *et al.* Defective valvulogenesis in HB-EGF and TACE-null mice is associated with aberrant BMP signaling. EMBO J 2003; 22:2704–2716.
20 Nakamura Y, Handa K, Iwamoto R, *et al.* Immunohistochemical distribution of CD9, heparin binding epidermal growth factor-like growth factor, and integrin alpha3beta1 in normal human tissues. J Histochem Cytochem 2001;49:439–444.
21 Fujino T, Hasebe N, Fujita M, *et al.* Enhanced expression of heparin-binding EGF-like growth factor and its receptor in hypertrophied left ventricle of spontaneously hypertensive rats. Cardiovasc Res 1998; 38:365–374.
22 Iwabu A, Murakami T, Kusachi S, *et al.* Concomitant expression of heparin-binding epidermal growth factor-like growth factor mRNA and basic fibroblast growth factor mRNA in myocardial infarction in rats. Basic Res Cardiol 2002;97:214–222.
23 Tanaka N, Masamura K, Yoshida M, *et al.* A role of heparin-binding epidermal growth factor-like growth factor in cardiac remodeling after myocardial infarction. Biochem Biophys Res Commun 2002;297: 375–381.
24 Asakura M, Kitakaze M, Takashima S, *et al.* Cardiac hypertrophy is inhibited by antagonism of ADAM12 processing of HB-EGF: metalloproteinase inhibitors as a new therapy. Nat Med 2002;8:35–40.
25 Shah BH, Catt KJ. A central role of EGF receptor transactivation in angiotensin II-induced cardiac hypertrophy. Trends Pharmacol Sci 2003;24:239–244.
26 Taniyama Y, Morishita R, Aoki M, *et al.* Angiogenesis and antifibrotic action by hepatocyte growth factor in cardiomyopathy. Hypertension 2002;40:47–53.
27 Li Y, Takemura G, Kosai K, *et al.* Postinfarction treatment with an adenoviral vector expressing hepatocyte growth factor relieves chronic left ventricular remodeling and dysfunction in mice. Circulation 2003; 107:2499–2506.
28 Li Q, Li B, Wang X, *et al.* Overexpression of insulin-like growth factor-1 in mice protects from myocyte death after infarction, attenuating ventricular dilation, wall stress, and cardiac hypertrophy. J Clin Invest 1997;100:1991–1999.
29 Su EJ, Cioffi CL, Stefansson S, *et al.* Gene therapy vector-mediated expression of insulin-like growth factors protects cardiomyocytes from apoptosis and enhances neovascularization. Am J Physiol Heart Circ Physiol 2003;284:H1429–H1440.
30 Chen SH, Chen XH, Wang Y, *et al.* Combination gene therapy for liver metastasis of colon carcinoma *in vivo*. Proc Natl Acad Sci USA 1995;92:2577–2581.
31 Terazaki Y, Yano S, Yuge K, *et al.* An optimal therapeutic expression level is crucial for suicide gene therapy for hepatic metastatic cancer in mice. Hepatology 2003;37:155–163.
32 Aoyama T, Takemura G, Maruyama R, *et al.* Molecular mechanisms of non-apoptosis by Fas stimulation alone versus apoptosis with an additional actinomycin D in cultured cardiomyocytes. Cardiovasc Res 2002;55: 787–798.
33 Ogasawara J, Watanabe-Fukunaga R, Adachi M, *et al.* Lethal effect of the anti-Fas antibody in mice. Nature 1993;364:806–809.
34 Takemura G, Kato S, Aoyama T, *et al.* Characterization of ultrastructure and its relation with DNA fragmentation in Fas-induced apoptosis of cultured cardiac myocytes. J Pathol 2001;193:546–556.
35 Toraason M, Wey H, Woolery M, *et al.* Arachidonic acid supplementation enhances hydrogen peroxide induced oxidative injury of neonatal rat cardiac myocytes. Cardiovasc Res 1995;29:624–628.
36 Villarreal FJ, Kim NN, Ungab GD, *et al.* Identification of functional angiotensin II receptors on rat cardiac fibroblasts. Circulation 1993;88:2849–2861.
37 Takemura G, Ohno M, Hayakawa Y, *et al.* Role of apoptosis in the disappearance of infiltrated, proliferated interstitial cells after myocardial infarction. Circ Res 1998;82:1130–1138.
38 Leor J, Quinones MJ, Patterson M, *et al.* Adenovirus-mediated gene transfer into infarcted myocardium: feasibility, timing, and location of expression. J Mol Cell Cardiol 1996;28:2057–2067.
39 Barr E, Carroll J, Kalynych AM, *et al.* Efficient catheter-mediated gene transfer into the heart using replication-defective adenovirus. Gene Therapy 1994;1:51–58.
40 Chu D, Sullivan CC, Weitzman MD, *et al.* Direct comparison of efficiency and stability of gene transfer into the mammalian heart using adeno-associated virus versus adenovirus vectors. J Thorac Cardiovasc Surg 2003;126:671–679.
41 Huang CY, Hao LY, Buetow DE. Insulin-like growth factor-induced hypertrophy of cultured adult rat cardiomyocytes is L-type calcium-channel-dependent. Mol Cell Biochem 2002;231:51–59.
42 Michalsky MP, Kuhn A, Mehta V, *et al.* Heparin-binding EGF-like growth factor decreases apoptosis in intestinal epithelial cells *in vitro*. J Pediatr Surg 2001;36:1130–1135.
43 Siddiqui AJ, Blomberg P, Wardell E, *et al.* Combination of angiopoietin-1 and vascular endothelial growth factor gene therapy enhances arteriogenesis in the ischemic myocardium. Biochem Biophys Res Commun 2003;310:1002–1009.

Research Article

Survivin-Responsive Conditionally Replicating Adenovirus Exhibits Cancer-Specific and Efficient Viral Replication

Junichi Kamizono,[1,3] Satoshi Nagano,[1,2,3] Yoshiteru Murofushi,[1] Setsuro Komiya,[3] Hisayoshi Fujiwara,[4] Toyojiro Matsuishi,[1,2] and Ken-ichiro Kosai[1,2]

[1]Division of Gene Therapy and Regenerative Medicine, Cognitive and Molecular Research Institute of Brain Diseases and [2]Department of Pediatrics and Child Health, Kurume University, Kurume, Japan; [3]Department of Orthopaedic Surgery, Graduate School of Medical and Dental Sciences, Kagoshima University, Kagoshima, Japan; and [4]Department of Cardiology, Respiratory and Nephrology, Regeneration and Advanced Medical Science, Graduate School of Medicine, Gifu University, Gifu, Japan

Abstract

Although a conditionally replicating adenovirus (CRA) exhibiting cancer-selective replication and induction of cell death is an innovative potential anticancer agent, current imperfections in cancer specificity and efficient viral replication limit the usefulness of this technique. Here, we constructed *survivin*-responsive CRAs (Surv.CRAs), in which expression of the wild-type or mutant adenoviral early region 1A (*E1A*) gene is regulated by the promoter of *survivin*, a new member of the inhibitor of apoptosis gene family. We explored the cancer specificity and effectiveness of viral replication of Surv.CRAs, evaluating their potential as a treatment for cancer. The *survivin* promoter was strongly activated in all cancers examined at levels similar to or even higher than those seen for representative strong promoters; in contrast, low activity was observed in normal cells. Surv.CRAs efficiently replicated and potently induced cell death in most types of cancer. In contrast, minimal viral replication in normal cells did not induce any detectable cytotoxicity. A single injection of Surv.CRAs into a preestablished tumor expressing *survivin*, even at relatively low levels, induced significant tumor death and inhibition of tumor growth. Furthermore, Surv.CRAs were superior to telomerase-dependent CRAs, one of the most effective CRAs that have been examined to date, both in terms of cancer specificity and efficiency. Thus, Surv.CRAs are an attractive potential anticancer agent that could effectively and specifically treat a variety of cancers. (Cancer Res 2005; 65(12): 5284-91)

Introduction

Conditionally replicating adenoviruses (CRAs), which selectively replicate in and kill tumor cells, may be an attractive tool for innovative cancer therapy (1). Achievement of both cancer specificity and efficient viral replication is critical for any CRA-oriented strategy. The CRAs that have been reported to date can primarily be classified into one of two groups (1). The first category employs the strategy of attenuating viral replication in normal cells by mutating cell cycle–inducing adenoviral genes necessary for viral replication; representatives of this group are the mutant type (MT) adenoviruses lacking an RB-binding site within early region 1A (E1A) and the MT adenoviruses lacking a p53-binding protein encoded by the early region 1B (*E1B*)-55K gene (2–4). Although these CRAs exhibit potential in cancer cells, these viruses do replicate and cause some cytopathic effects in normal cells (4–6). The second group of CRAs alters the regulation of E1A expression. *E1A* is the first gene to be transcribed after infection with wild-type (WT) adenoviruses, transactivating the viral and cellular genes critical for producing infective adenoviruses. CRAs of this category reproduce in a tumor-specific manner by replacing the native E1A promoter with a tissue- and tumor-specific promoter, such as the prostate-specific antigen promoter (7), the α-fetoprotein promoter (8), the midkine promoter (9), or the tyrosinase promoter (10). Although previous studies of this CRA strategy have been promising, the use of tissue-specific promoters has the disadvantage of targeting only limited types of cancer. In addition, these promoters show insufficient cancer specificity (leaky transactivation in normal cells) and weak activity even in cancer cells. Thus, viral targeting and replication for previously reported CRAs may not have achieved sufficient efficiency or cancer specificity. The use of a novel and ideal promoter able to induce strong expression in a cancer-specific manner is crucial to circumventing these problems.

Survivin, a new member of the inhibitor of apoptosis gene family, was reported to be expressed in high levels in cancerous but not normal tissues (11). Clinical studies have indicated a positive correlation between high *survivin* expression levels and a poor prognosis, an accelerated rate of recurrence, and an increased resistance to therapy in cancer patients (12). *Survivin* is predominantly expressed during the G_2-M phase of the cell cycle, functioning in mitosis via interactions with microtubules (13). In addition, the *survivin* promoter successfully regulates transgene expression in a cancer-specific manner (14). Moreover, studies have suggested that a putative region of the *survivin* promoter is likely responsible for the induction of cancer-specific expression in tumors at high levels (15, 16). The promoter contains multiple cell cycle–dependent elements and a cell cycle gene homology region, which may control expression of various G_2-M-regulated genes, including the *survivin* gene, in a manner correlating with G_2-M cell cycle periodicity (13, 15–17).

In this study, we generated and analyzed two *survivin*-responsive CRAs (Surv.CRAs). Surv.CRAwt and Surv.CRAmt expressed WT and MT E1A under the control of the *survivin* promoter, respectively. We finally compared these Surv.CRAs to a recently reported CRA, in which E1A is regulated by the telomerase reverse transcriptase (TERT) promoter (Tert.CRA), currently one of the best CRAs available (18–20).

Materials and Methods

Cell lines. The human cell lines MKN-1 and MKN-45 (gastric cancer cell lines); HCT-15, LoVo, and Colo-205 (colon cancer cell lines); HepG2 and

Note: J. Kamizono and S. Nagano contributed equally to this work.

Requests for reprints: Ken-ichiro Kosai, Division of Gene Therapy and Regenerative Medicine, Cognitive and Molecular Research Institute of Brain Diseases, Kurume University, 67 Asahi-machi, Kurume, 830-0011, Japan. Phone: 81-942-31-7910; Fax: 81-942-31-7911; E-mail: kosai@med.kurume-u.ac.jp.

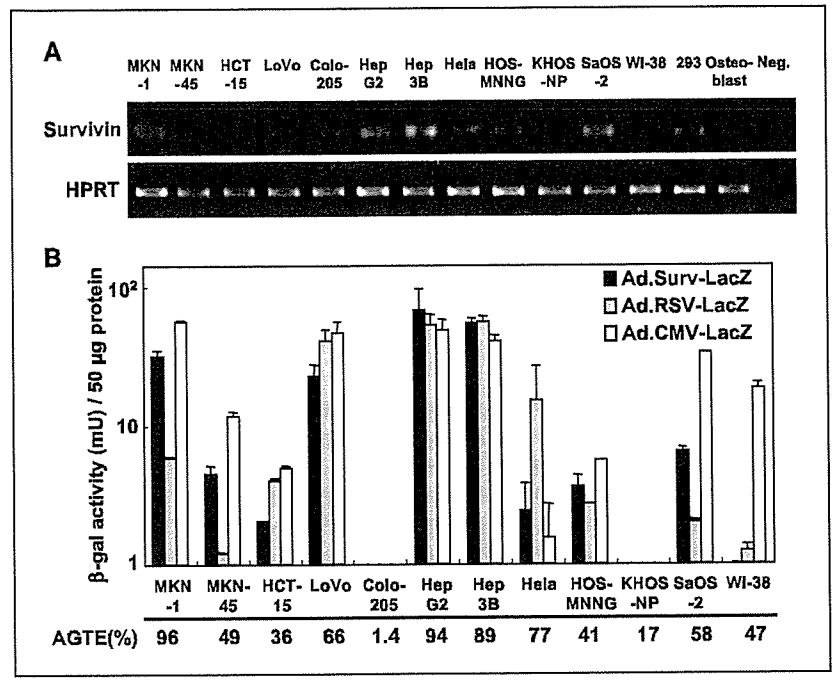

Figure 1. *Survivin* mRNA expression (*A*) and promoter activity (*B*). *A*, endogenous *survivin* mRNA was detected by PCR. The *HPRT* gene was amplified as an internal control. *Neg*, template was omitted from the reaction as a negative control. *B*, β-gal enzyme activity was detected 48 hours after infection with Ad.Surv-LacZ, Ad.CMV-LacZ, or Ad.RSV-LacZ at an MOI of 30. *Columns*, mean of three independent experiments; *bars*, ±SE. AGTE is presented as the percentage of X-gal-stained cells observed among the total cells at 48 hours after Ad.CMV-LacZ infection at an MOI of 30.

Hep3B (hepatoma cell lines); HeLa (a cervical cancer cell line); SaOS-2, HOS-MNNG, and KHOS-NP (osteosarocoma cell lines); and WI-38 (a primary lung fibroblast) were maintained in DMEM supplemented with penicillin/streptomycin and 10% fetal bovine serum. Primary human osteoblasts, obtained from Bio Whittaker (Walkersville, MD), were maintained according to the manufacturer's protocol.

Generation of adenoviruses. A region of the mouse *survivin* gene promoter (−173 to −19), which contains two cell cycle–dependent elements and one cell cycle gene homology region, was obtained from mouse genomic DNA by PCR using the following primers: sense (S)-Surv.pr 5′-AGATGGGCGTGGGGCGGGAC-3′ and antisense (AS)-Surv.pr 5′-TCCGCCAAGACGACTCAAAC-3′. Generation of Surv.CRAwt, Surv.CRAmt, and Tert.CRAwt viruses, which contained WT or MT E1A downstream of either the *survivin* or TERT promoter (−181 to +79; kindly provided by Dr. S. Kyo, Kanazawa University School of Medicine; ref. 21), E1BΔ55K downstream of the cytomegalovirus immediate-early gene enhancer/promoter (CMV promoter), and the enhanced green fluorescent protein (*EGFP*) gene downstream of the CMV promoter, was done using a novel method developed by our group (22).

An E1-deleted replication-defective adenovirus expressing EGFP (Ad.ΔE1) and E1-deleted adenoviruses expressing the *LacZ* gene under the control of the Rous sarcoma virus long-terminal repeat (RSV promoter), the CMV promoter, the *survivin* promoter, or the TERT promoter (Ad.RSV-LacZ, Ad.CMV-LacZ, Ad.Surv-LacZ, and Ad.Tert-LacZ, respectively) were generated and prepared as described previously (23).

Reverse transcription-PCR analysis. Extraction of total RNA from the cells and the semiquantitative reverse transcription-PCR (RT-PCR) analyses were done as described previously (24), with the following primer sets and annealing temperatures: S-Surv 5′-CCCTTGGTGAATTTTTGAAA-3′ and AS-Surv 5′-TGGTGCCACTTTCAAGACAA-3′ for human *survivin* at 56°C; S-TERT 5′-TTCCTGCACTGGCTGATGAGTGT-3′ and AS-TERT 5′-CGCTCGGCCCTCTTTTCTCTG-3′ for human *TERT* at 59°C (25); and S-HPRT 5′-CCTGCTGGATTACATTAAAGCACTG-3′ and AS-HPRT 5′-AAGGGCATATCCAACAACAA-3′ for hypoxanthine guanine phosphoribosyl transferase (*HPRT*) as an internal control at 57°C (24, 26).

Promoter activities and adenoviral gene transduction efficiency. Cells (5×10^5 cells per plate) were infected with Ad.CMV-LacZ, Ad.RSV-LacZ, Ad.Surv-LacZ, or Ad.Tert-LacZ at a multiplicity of infection (MOI) of 30 for 24 hours. After harvesting, cellular β-galactosidase (β-gal) activity was measured as previously described (27).

The adenoviral gene transduction efficiency (AGTE) for each cell *in vitro* was determined 48 hours after infection with Ad.CMV-LacZ at an MOI of 30, as previously described (27–29).

Flow cytometric analysis. After infection with each adenovirus, cells were detached with trypsin and fixed in 4% paraformaldehyde. The percentage of EGFP-positive cells was then analyzed by flow cytometry on a FACSCalibur using CELLQuest software (Becton Dickinson, San Jose, CA).

Cytotoxic effects *in vitro*. After plating in 96-well plates, cells were infected with each adenovirus at a variety of MOIs. Cell viability was determined 3 and 5 days after adenoviral infection using a WST-8 assay (Dojindo Laboratories, Mashiki, Japan) according to the manufacturer's protocol.

Therapeutic effects *in vivo* in animal experiments. HOS-MNNG cells (5×10^6 cells) were injected s.c. into the back of 5-week-old male BALB/c athymic nude mice. After the s.c. tumors reached 6 to 10 mm in diameter, the mice were randomly divided into three groups. Each group was given a single injection of 1×10^8 plaque-forming unit (pfu) Surv.CRAwt ($n = 9$), Surv.CRAmt ($n = 8$), or Ad.ΔE1 ($n = 8$) in 50 μL of 10 mmol/L Tris-HCl (pH 7.4)/1 mmol/L $MgCl_2$/10% (v/v) glycerol/hexadimethrine bromide (20 μg/mL) into the s.c. tumor. In another comparative experiment, tumor-bearing mice were infected with Tert.CRAwt ($n = 9$), Surv.CRAwt ($n = 8$), or Ad.ΔE1 ($n = 11$) as described above. Tumor size was then monitored twice a week using digital calipers. Tumor volume was calculated according to the following formula: volume = long axis × (short axis)^2 × 0.5 (29, 30).

For histopathologic analysis, the tumors were fixed in 10% buffered formalin, embedded in paraffin, cut into 4-μm serial sections, and stained with H&E.

The protocol for this animal experiment was approved by the Animal Research Committee of Kurume University. All animal experiments were done in accordance with the NIH Guidelines for the Care and Use of Laboratory Animals.

Statistical analysis. Data are represented as the means ± SE. Statistical significance was determined using the Student's *t* test. $P < 0.05$ were considered to indicate statistical significance.

Results

***Survivin* mRNA was expressed in various cancer cell lines.** The RT-PCR analyses showed that *survivin* mRNA was expressed in multiple cancer cells derived from a variety of tissue origins;

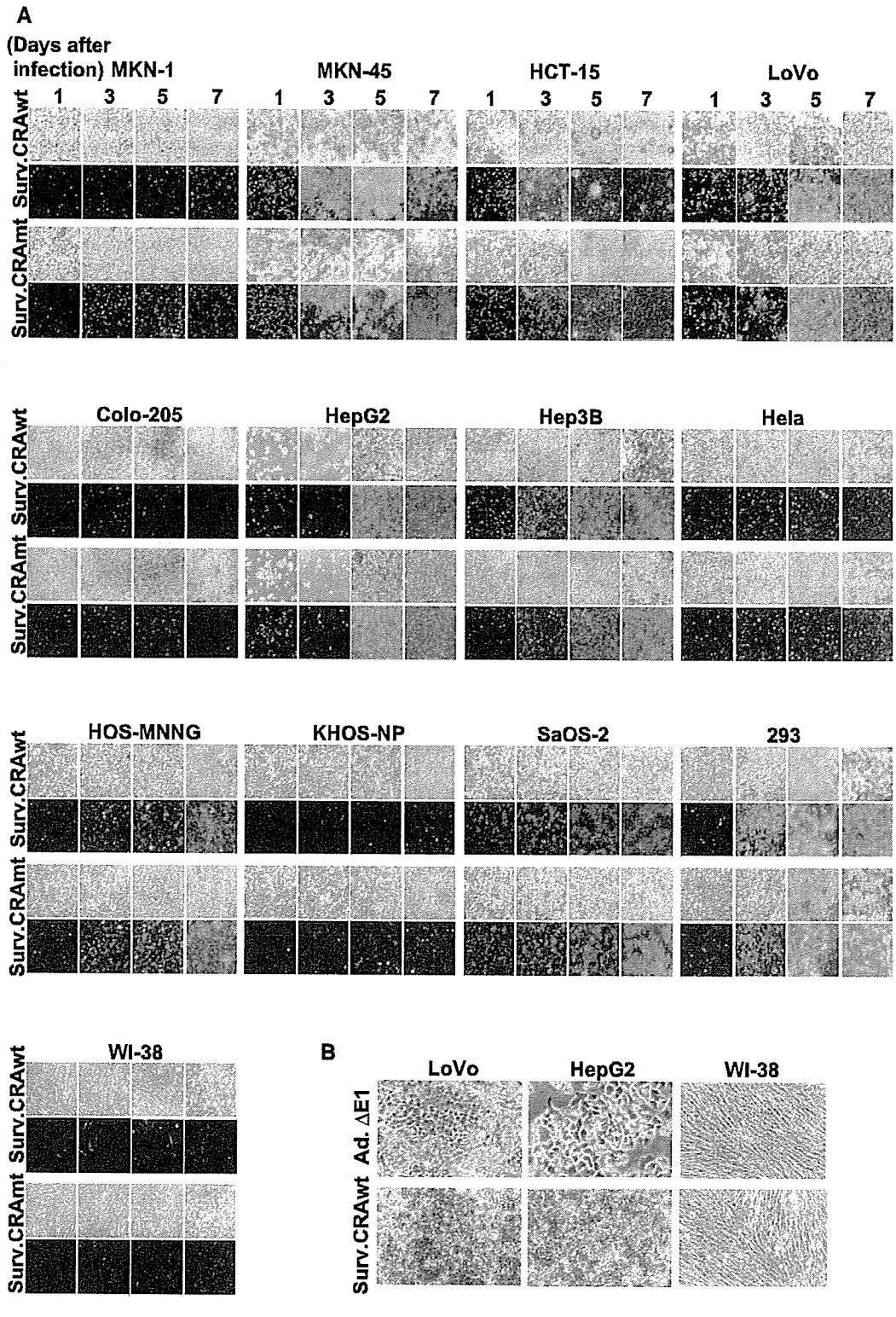

Figure 2. Replication and cytotoxicity of Surv.CRAs in different cell lines. *A*, representative phase-contrast (*top*) and fluorescent microscopic images (*bottom*) 1, 3, 5, and 7 days after infection with Surv.CRAwt or Surv.CRAmt at an MOI of 0.1. EGFP-positive cells increased in a time-dependent manner after infection with either Surv.CRAwt or Surv.CRAmt in all cancer cells examined; in contrast, no significant increases in EGFP-positive cells were observed in normal WI-38 cells. The rate of spreading of EGFP-positive cells and CPE correlated well with the endogenous levels of expression of *surivin* and the AGTE levels, as shown in Fig. 1. *B*, a high-power phase-contrast microscopic image taken 7 days after infection with control Ad.ΔE1 or Surv.CRAwt showed that all of the LoVo and HepG2 cells underwent cytopathic effect after infection with Surv.CRAwt only. In contrast, no cytopathic effect was observed in WI-38 cells after infection with either adenovirus.

this finding was consistent with previous reports (ref. 11; Fig. 1*A*). The levels of *survivin* mRNA, however, varied widely among the different cancer cell lines. *Survivin* mRNA expression was remarkably high in both hepatoma cell lines tested, HepG2 and Hep3B, and in one of the osteosarcoma cell lines, SaOS-2. The levels in the other cell lines were only moderate or relatively low. *Survivin* mRNA was also detected in normal WI-38 human fibroblasts and primary human osteoblasts; these levels, however, were relatively low in comparison to those seen in the cancer cell lines.

Strong cancer-specific activity of the *survivin* promoter. The *survivin* promoter provided strong transcriptional activation in all of the cancer cell lines that showed sufficient viral transduction (Fig. 1*B*). The low levels or absence of β-gal activity after infection with adenoviruses in either Colo-205 or KHOS-NP cells was apparently due to very low levels of AGTE in these cells and not to a low activity of the *survivin* promoter. β-gal activity was not detected in this group even after infection with Ad.RSV-LacZ or Ad.CMV-LacZ at the same MOI (MOI of 30). The apparent variability in β-gal levels was also due to both the variability of AGTE levels in individual cells and the cellular activity required to express the transgenes and not the variability in *survivin* promoter activity. In seven of the remaining nine cancer cell lines, the *survivin* promoter exhibited stronger activity than either the RSV promoter or the CMV promoter, two representative ubiquitously strong promoters (27, 28). Notably, the *survivin* promoter was stronger than both the RSV and CMV promoters in HepG2 cells. In two additional cell lines, HCT-15 and LoVo, the *survivin* promoter displayed activity levels very similar to those observed for the RSV and CMV promoters.

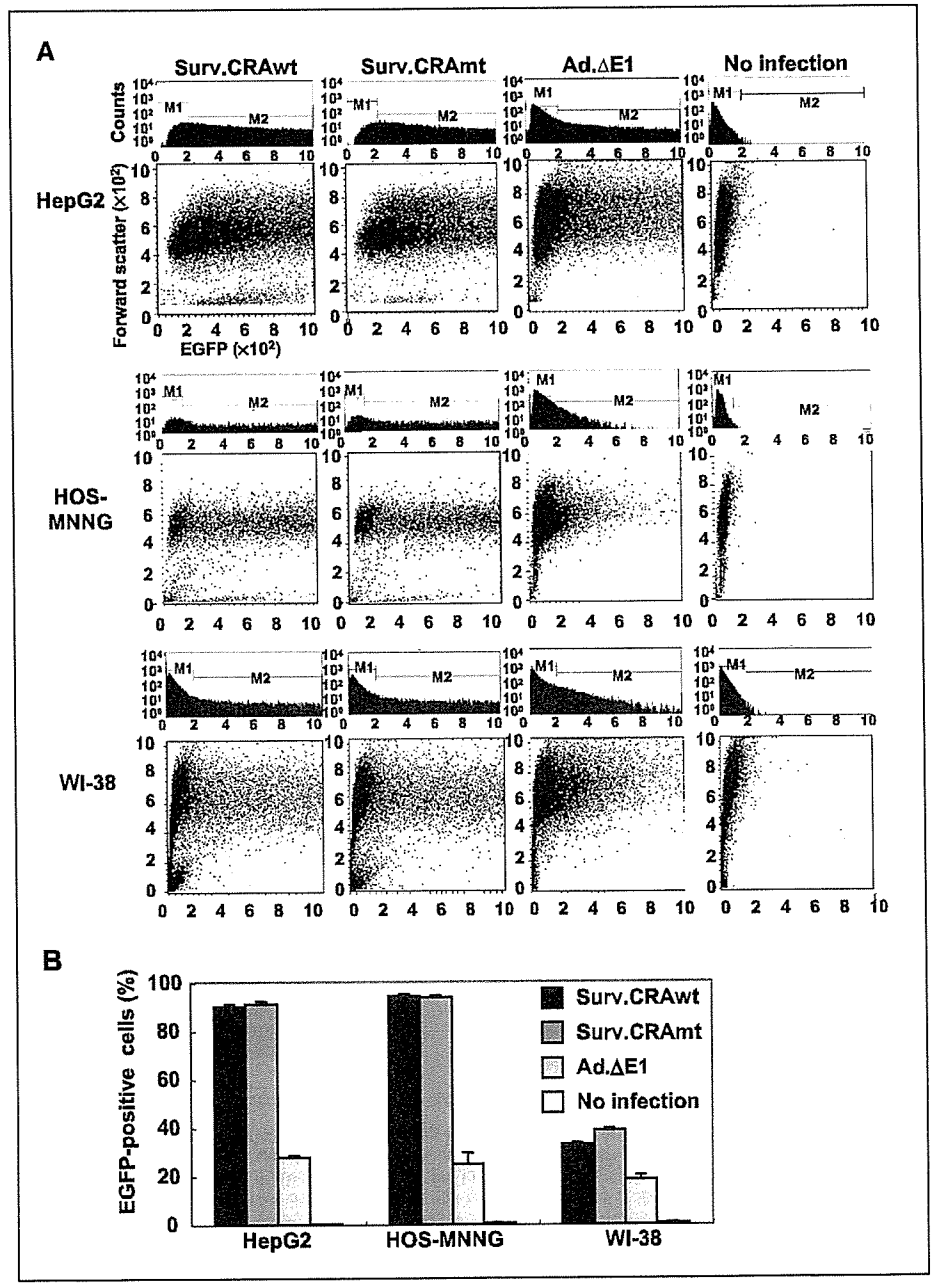

Figure 3. Flow cytometric analysis of EGFP-positive cells. HepG2, HOS-MNNG, and WI-38 cells were infected with Surv.CRAwt, Surv.CRAmt, or Ad.ΔE1 at an MOI of 0.1 (HepG2) or 1 (HOS-MNNG and WI-38). Twenty-four hours later, cells were fixed with 4% paraformaldehyde; the percentage of EGFP-positive cells was analyzed by flow cytometry. *A*, histograms (*top*) of EGFP-positive cells (M1, negative; M2, positive) and dot plots (*bottom*) individually representing the EGFP intensity and the forward scatter index. *B*, *columns*, percentages of EGFP-positive cells (mean of three independent experiments); *bars*, ±SE.

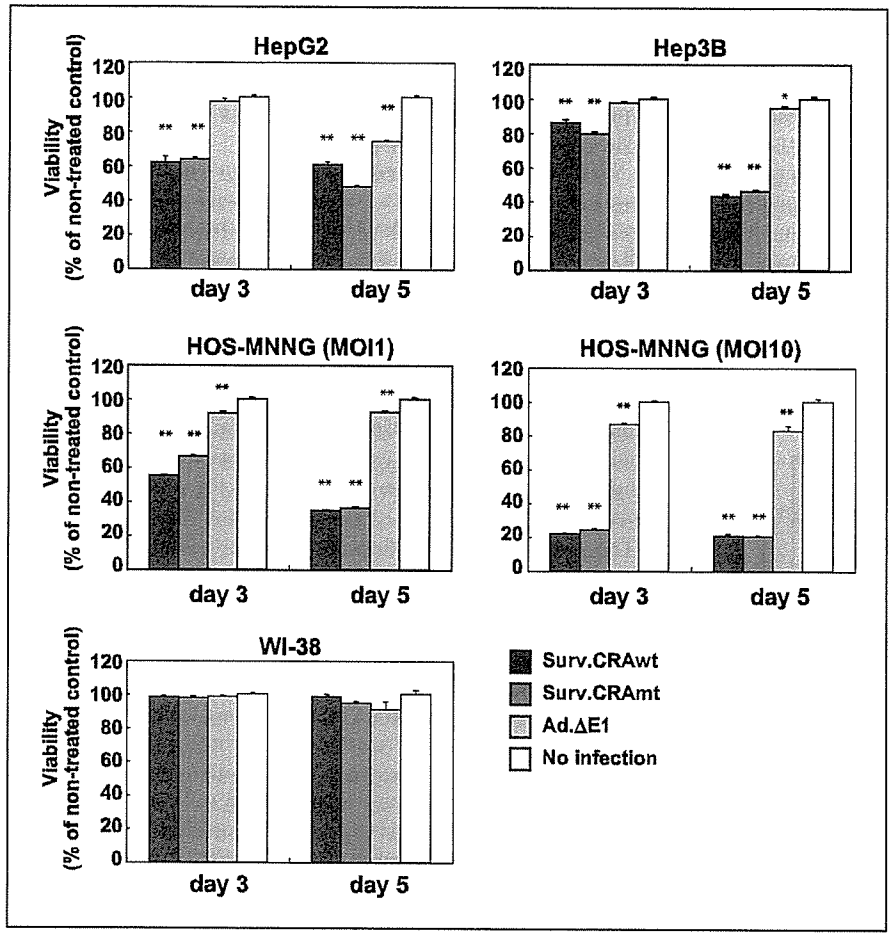

Figure 4. Cytotoxic effects *in vitro*. Cells were infected with Surv.CRAwt, Surv.CRAmt, or Ad.ΔE1 at an MOI of 0.1 in HepG2 and Hep3B cells, MOIs of 1 and 10 in HOS-MNNG cells, and an MOI of 1 in WI-38 cells. Cell viability was determined by WST-8 assay 3 or 5 days after infection. *, $P < 0.05$ and **, $P < 0.001$ (statistical significance in comparison with the no-infection control).

In contrast, *survivin* promoter activity was not detected in normal WI-38 fibroblasts despite both high levels of RSV and CMV promoter activity and moderate to high AGTE levels. Despite detectable, albeit low, levels of endogenous *survivin* expression, no detectable transactivation could be observed in normal cells with the use of this *survivin* promoter (Fig. 1*B*). Thus, the *survivin* promoter region and length of the transcriptional regulatory element used in these experiments are suitable to induce strong transactivation in all cancer types examined here in a tumor-specific manner.

Surv.CRAs efficiently and selectively replicated in cancer. After infection with Surv.CRAwt or Surv.CRAmt, the number of EGFP-positive cells increased in a time-dependent manner in all of the cancer cell lines analyzed, indicating the efficient replication of both Surv.CRAs (Fig. 2). Cytopathic effect was efficiently induced within a short period of time after the appearance of EGFP positivity. The speed of the Surv.CRA spreading was consistent with the observed levels of β-gal activity (Fig. 1*B*), except for MKN-45 cells. In these cells, the Surv.CRAs replicated very rapidly, spreading throughout the entire culture dish at a rate similar to that seen in LoVo, HepG2, and Hep3B cells. The slow yet still apparent spread of the Surv.CRAs was even observed in Colo-205 cells, despite a low AGTE in the initial infection. This phenomenon likely results from high levels of endogenous *survivin* expressed, suggesting that efficient viral replication within cells may overcome the disadvantage of low AGTE. In contrast, the percentage of EGFP-positive cells did not clearly increase over a 7-day period in normal WI-38 cells, although the EGFP fluorescence intensity within each cell increased minimally. In addition, no cytopathic effect was observed in WI-38 cells even at 7 days after infection with Surv.CRAs.

To verify tumor-specific replication of both Surv.CRAs accurately and quantitatively, we did flow cytometric analysis using two representative cancer cell lines, HepG2 and HOS-MNNG, as well as normal WI-38 cells. HepG2 cells exhibited the highest levels of *survivin* expression, the highest AGTE levels, and the strongest *survivin* promoter activity, resulting in rapid amplification of the Surv.CRAs (Fig. 2). HOS-MNNG showed low to moderate levels of these properties, resulting in lower but significant viral replication. Twenty-four hours after infection with either of the adenoviruses at the MOI that initially provided approximately 20% AGTE, Surv.CRAs propagated rapidly, spreading to >90% of HepG2 and HOS-MNNG cells. Under these conditions, we could not observe any significant amplification or spread of the control replication-defective Ad.ΔE1 (Fig. 3). In contrast, the propagation and resulting spread of Surv.CRAs remained minimal in WI-38 cultures. Thus, both Surv.CRAs replicated more efficiently in cancer cells, even those expressing *survivin* at relatively low levels, with moderate AGTE levels, than in normal WI-38 cells. In addition, we did not detect any significant differences in the phenotypic characteristics of Surv. CRAwt and Surv.CRAmt in any of the cell types tested.

Surv.CRAs specifically kill cancer cells *in vitro*. To assess the selective killing of cancer cells by Surv.CRAs, we conducted a cell viability assay (Fig. 4). In two representative cell lines showing both high AGTE and high levels of *survivin* expression, HepG2 and Hep3B cells, Surv.CRAs induced prominent cytotoxic effects as

early as 3 days, even when infection was done at a low MOI (0.1). Both hepatoma cell lines were sensitive to adenoviral cytotoxicity; cytotoxic effects were minimally but clearly seen 5 days after infection at an MOI of 0.1 with the control, E1-deleted Ad.ΔE1. In HOS-MNNG cells, which exhibited low expression of *survivin* and moderate AGTE levels, both Surv.CRAs induced more prominent cytotoxicity than Ad.ΔE1. The cytotoxic effects were amplified in a dose-dependent manner when initial infection at increasingly higher MOI (Fig. 4). In contrast to these results in cancer cell lines, neither Surv.CRA induced cytotoxic effects in normal WI-38 fibroblast cells, even 5 days after infection at an MOI of 1. Thus, both Surv.CRAs efficiently induced cell death in three cancer cell lines in contrast to the lack of clear toxicity observed in normal WI-38 cells. In addition, we did not observe any significant differences in the cytotoxicity of Surv.CRAwt and Surv.CRAmt between the cell types tested, including the normal WI-38 cells, RB-intact HepG2 cells, and RB-deficient Hep3B cells.

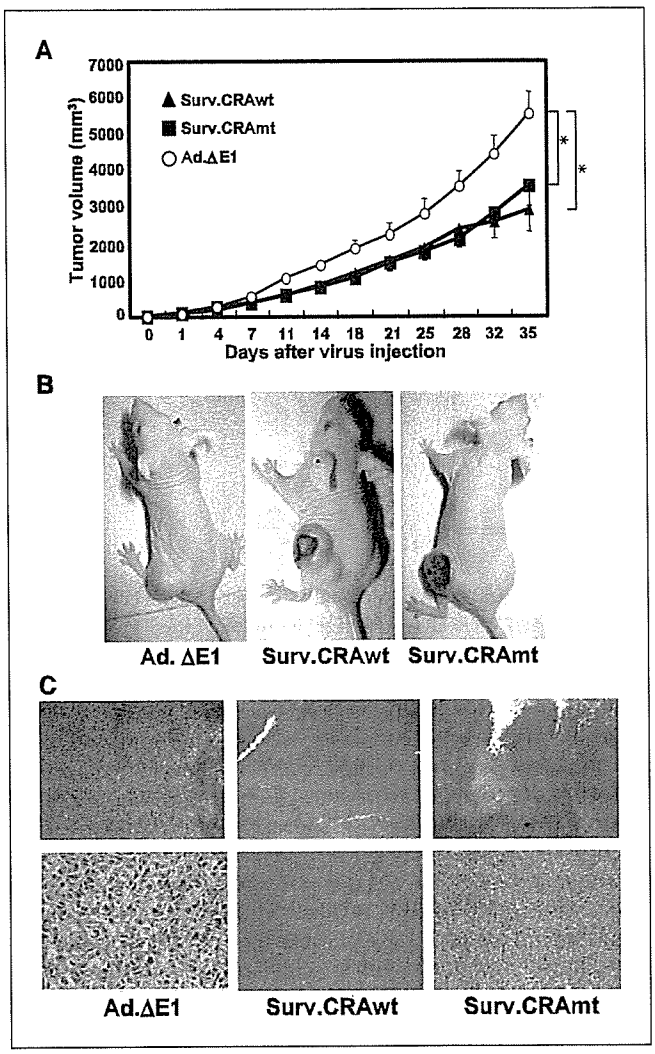

Figure 5. Therapeutic effects of Surv.CRAs *in vivo*. *A*, tumor volume was measured after a single injection of 1×10^8 pfu Surv.CRAwt ($n = 9$), Surv.CRAmt ($n = 8$), or control Ad.ΔE1 ($n = 8$) into preestablished s.c. tumors of HOS-MNNG cells in nude mice. *, $P < 0.05$ (statistical significance in comparison with infection with the control Ad.ΔE1). *B*, representative macroscopic pictures 14 days after injection of Ad.ΔE1, Surv.CRAwt, or Surv.CRAmt. Prominent tumor necrosis was apparent in Surv.CRAwt- and Surv.CRAmt-treated masses. *C*, representative histologic images at the time of sacrifice. H&E-stained sections exhibited large necrotic areas in the tumor nodules in mice treated with either Surv.CRA. In contrast, tumor nodules contained primarily viable tumor cells without large necrotic areas in the Ad.ΔE1-treated mice. Original magnification: ×20 (*top*) and ×100 (*bottom*). Both the macroscopic and microscopic pictures provide a more accurate assessment of the therapeutic potential of the Surv.CRAs than the simple assessment of tumor volume.

Surv.CRA inhibited tumor growth *in vivo*. Using an animal model of preestablished s.c. tumors, we examined the therapeutic potential of both Surv.CRAs *in vivo*. We intentionally used an HOS-MNNG osteosarcoma cell line that expressed relatively low levels of *survivin* and showed moderate levels of AGTE to assess the therapeutic potentials of these vectors in a wider range of cancers. A single intratumoral administration (1×10^8 pfu) of Surv.CRAwt or Surv.CRAmt significantly inhibited tumor growth in comparison to the same dose of Ad.ΔE1 (Fig. 5*A*). Statistically significant differences in the tumor size were seen between Surv.CRAs-treated and Ad.ΔE1-treated mice as early as 11 days after administration and continuing thereafter. As assessed by macroscopic and microscopic examination, the therapeutic effects of both Surv.CRAs were more significant; the tumor nodules in Surv.CRA-treated mice contained large necrotic areas, whereas the nodules in Ad.ΔE1-treated mice consisted primarily of viable tumor cells histologically showing active malignant features (Fig. 5*B* and *C*). These results suggest the therapeutic potential and general utility of Surv.CRAs for the treatment of cancer.

The superiority of Surv.CRAs to a Tert.CRA. We compared the viral properties of Surv.CRAs with those of Tert.CRA. The expression levels of endogenous TERT varied among cancer cell lines; HOS-MNNG cells, as well as HepG2 cells, expressed TERT mRNA at very high levels (Fig. 6*A*), in contrast to the relatively low level of *survivin* expression in HOS-MNNG cells (Fig. 1*A*). Nevertheless, the activity of the *survivin* promoter in HOS-MNNG cells was higher than that of the TERT promoter, as well as in HepG2 cells (Fig. 6*B*). These results suggest that the *survivin* promoter may be more active than the TERT promoter among multiple cancer cell types.

To precisely analyze the differences in the efficiency and attenuation of viral replication between Surv.CRAs and Tert.CRA in cancerous and normal cells, we did flow cytometric analysis after infection of three types of cells at low MOI (Fig. 6*C*). Surv.CRAwt exhibits more efficient replication in both HepG2 and HOS-MNNG cells than that seen in Tert.CRAwt cells, although the former virus is more quiescent in normal WI-38 cells than the latter.

We compared the therapeutic potentials of Surv.CRAwt and Tert.CRAwt in tumor-bearing animals (Fig. 6*D*). Although we did not find a statistically significant difference in the effects of Surv.CRAwt and Tert.CRAwt, both viruses significantly decreased tumor size in animals from the tumor volumes observed in mice treated with the control Ad.ΔE1 virus. Tumor volumes in Surv.CRAwt-treated mice were smaller than those in Tert.CRAwt-treated animals; in addition, the difference between the Surv.CRAwt and control Ad.ΔE1 groups was more significant (smaller P) than the difference between the Tert.CRAwt and Ad.ΔE1 groups.

Discussion

This study provides the first report of two *survivin*-responsive CRAs, both showing efficient cancer-specific replication and potent therapeutic effects against cancers both *in vitro* and *in vivo*.

One of the attractive features of Surv.CRAs is their ability to target a variety of cancers. Surv.CRAs showed efficient propagation and induced cell death in a wide variety of tumor cells with a variety of

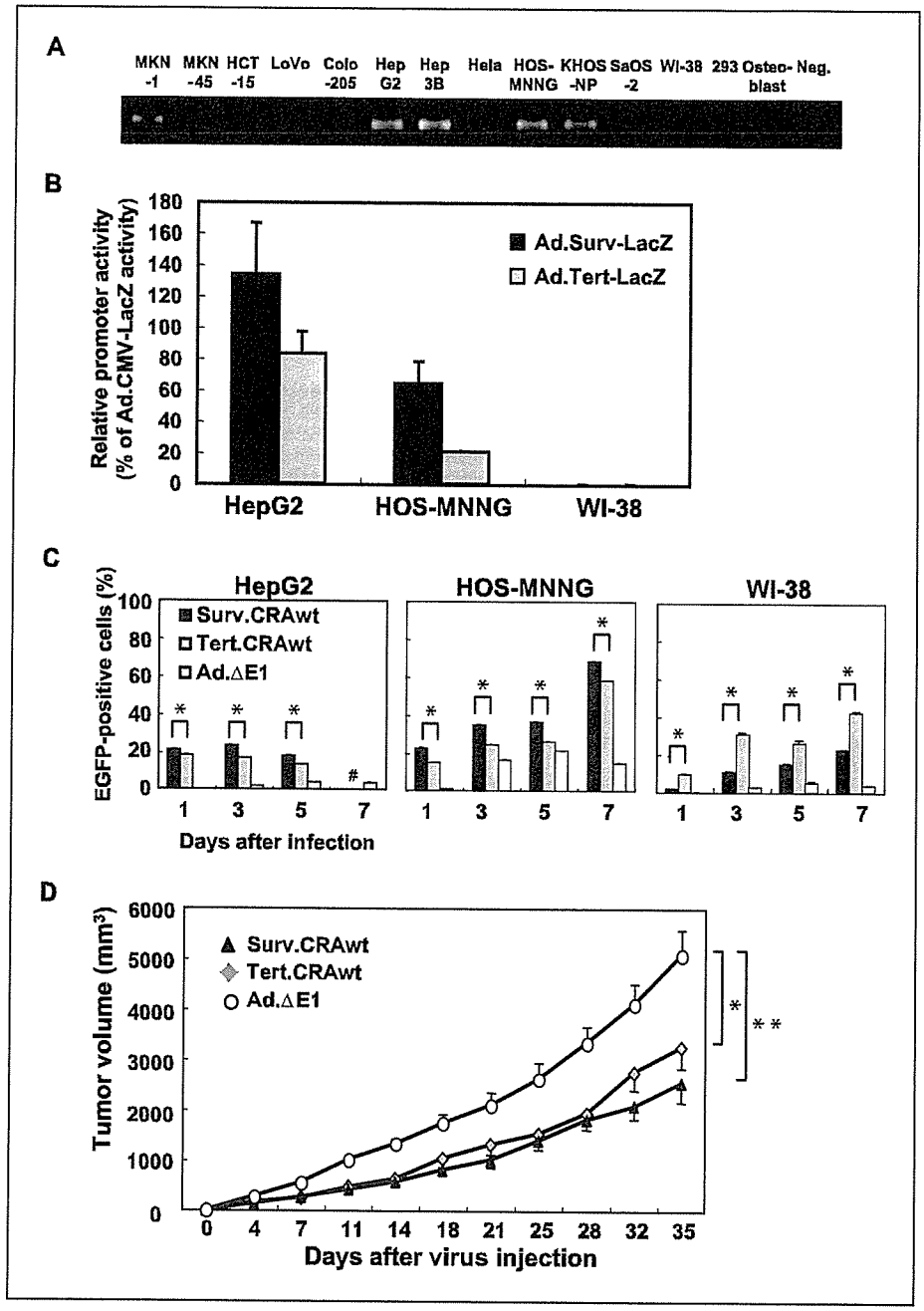

Figure 6. Comparison of Surv.CRA with Tert.CRA. *A,* endogenous TERT mRNA was detected by RT-PCR. *B,* relative activity of the *survivin* promoter and the TERT promoter to that of the CMV promoter. X-gal activity was determined 48 hours after infection with Ad.Surv-LacZ, Ad.Tert-LacZ, or Ad.CMV-LacZ at an MOI of 30. *C,* rate of viral propagation was assessed by flow cytometric analysis, expressed as the percentage of EGFP-positive cells 1, 3, 5, and 7 days after infection with either adenoviruses at an MOI of 0.03 in HepG2 cells and an MOI of 0.1 in HOS-MNNG and WI-38 cells. *, $P < 0.05$. Both Surv.CRAwt and Tert.CRAwt rapidly replicated between 5 and 7 days after infection of HepG2 cells at this MOI; infected cells detached from the culture dishes at seven days post infection (#). *D,* tumor volume was measured after a single injection of 1×10^8 pfu Surv.CRAwt ($n = 8$), Tert.CRAwt ($n = 9$), or control Ad.ΔE1 ($n = 11$) into preestablished s.c. HOS-MNNG tumors in nude mice. *, $P < 0.05$ and **, $P < 0.005$ (statistical significance in comparison with control Ad.ΔE1).

phenotypes, including low levels of *survivin* expression. The problem of low AGTE in certain cancer types is a critical issue in adenoviral gene therapy; Surv.CRAs are no exception. Further attempts should be made to improve adenoviral infectivity. Nevertheless, this study showed that Surv.CRAs propagated even in cell types with low AGTE values, a promising result for the potential of these vectors as therapeutic agents. In addition, we intentionally used HOS-MNNG cells, which express *survivin* at relatively low levels and exhibit only moderate AGTE, for *in vivo* animal studies. The anticancer effect of Surv.CRAs under these conditions suggests that this agent may elicit therapeutic effects in many cancer types. Moreover, recent studies have detailed promising approaches to overcome the obstacle of low AGTE, such as fiber modification (31–33); these techniques could be also be directly and feasibly applied to Surv.CRAs (22). Fiber-modified Surv.CRA may enhance the cancer specificity and efficacy of this therapy for a broader range of cancer types and should be explored further.

Another crucial requirement for optimal CRA is attenuation of viral replication in normal cells. Currently, one of the best available CRAs may be Tert.CRA; TERT, the major determinant of telomerase activity, is expressed at high levels in many cancer cells but not in normal cells (34). Several recent studies have shown cancer-selective replication and anticancer effects of Tert.CRAs (18–20). After examining the endogenous expression levels and promoter activity of TERT in a variety of cancer and normal cells, we compared the viral replication of Surv.CRAwt to that of Tert.CRAwt in both cancer and normal cells. Surv.CRAwt showed greater promise; the replication of Surv.CRAs in normal cells was more

attenuated than that of the Tert.CRA, whereas Surv.CRAwt was more efficient in replicating in two independent cancer cell types, including HOS-MNNG. As HOS-MNNG expressed *survivin* and TERT at low and high levels, respectively, it is likely that Surv.CRAs are superior to Tert.CRAs in both cancer specificity and efficiency, although the general applicability of this trend will need to be confirmed in future studies.

Previous studies have not yet explored whether deletion of the RB-binding domain when combined with the modulation of E1A expression using a tumor-specific promoter provides additional advantages or disadvantages over either approach alone (4). In this study, Surv.CRAmt did not provide an enhanced cancer specificity or an attenuation of viral replication in normal cells but also do not reduce viral replication in the cancer cells examined, including both RB-deficient and RB-intact tumor cells and normal fibroblast cells. The *survivin* promoter may confer such a high level of cancer specificity that these additional viral modifications do not provide a clear additional advantage. It is also possible that both RB-dependent and *survivin*-dependent cancer specificities target cell cycle dysregulation; therefore, the cancer specificity of RB- and *survivin*-dependent viruses may overlap to some extent. Future studies should be conducted to modify further the expression elements of other adenoviral genes using different promoters that target cancer-specific genetic events independent of cell cycle dysregulation, because the replication of Surv.CRAs in normal cells was greatly attenuated but not completely abrogated.

In conclusion, this study showed the therapeutic potential of *survivin*-responsive CRAs; these Surv.CRAs confer cancer-specific replication and cytotoxicity and thus may provide an attractive therapeutic agent for the treatment of cancer.

Acknowledgments

Received 7/26/2004; revised 3/30/2005; accepted 4/12/2005.

Grant support: A Grant-in-Aid for Scientific Research on Priority Areas (C); a grant for Cooperation of Innovative Technology and Advanced Research in Evolutional Area from the Ministry of Education, Culture, Sports, Science and Technology, Japan; and Health and Labour Sciences Research Grants for Third Term Comprehensive Control Research for Cancer from the Ministry of Health, Labour and Welfare, Japan.

The costs of publication of this article were defrayed in part by the payment of page charges. This article must therefore be hereby marked *advertisement* in accordance with 18 U.S.C. Section 1734 solely to indicate this fact.

We thank M. Saito and A. Kusano for their technical assistance, Dr. S. Kyo for providing the material, and David Cochran for editing the article.

References

1. Alemany R, Balague C, Curiel DT. Replicative adenoviruses for cancer therapy. Nat Biotechnol 2000;18:723–7.
2. Fueyo J, Gomez-Manzano C, Alemany R, et al. A mutant oncolytic adenovirus targeting the Rb pathway produces anti-glioma effect *in vivo*. Oncogene 2000; 19:2–12.
3. Bischoff JR, Kirn DH, Williams A, et al. An adenovirus mutant that replicates selectively in p53-deficient human tumor cells. Science 1996;274:373–6.
4. Heise C, Hermiston T, Johnson L, et al. An adenovirus E1A mutant that demonstrates potent and selective systemic anti-tumoral efficacy. Nat Med 2000;6:1134–9.
5. Rothmann T, Hengstermann A, Whitaker NJ, Scheffner M, zur Hausen H. Replication of ONYX-015, a potential anticancer adenovirus, is independent of p53 status in tumor cells. J Virol 1998;72:9470–8.
6. Harada JN, Berk AJ. p53-Independent and -dependent requirements for E1B-55K in adenovirus type 5 replication. J Virol 1999;73:5333–44.
7. Rodriguez R, Schuur ER, Lim HY, Henderson GA, Simons JW, Henderson DR. Prostate attenuated replication competent adenovirus (ARCA) CN706: a selective cytotoxic for prostate-specific antigen-positive prostate cancer cells. Cancer Res 1997;57:2559–63.
8. Hallenbeck PL, Chang YN, Hay C, et al. A novel tumor-specific replication-restricted adenoviral vector for gene therapy of hepatocellular carcinoma. Hum Gene Ther 1999;10:1721–33.
9. Adachi Y, Reynolds PN, Yamamoto M, et al. A midkine promoter-based conditionally replicative adenovirus for treatment of pediatric solid tumors and bone marrow tumor purging. Cancer Res 2001;61:7882–8.
10. Nettelbeck DM, Rivera AA, Balague C, Alemany R, Curiel DT. Novel oncolytic adenoviruses targeted to melanoma: specific viral replication and cytolysis by expression of E1A mutants from the tyrosinase enhancer/promoter. Cancer Res 2002;62:4663–70.
11. Ambrosini G, Adida C, Altieri DC. A novel anti-apoptosis gene, survivin, expressed in cancer and lymphoma. Nat Med 1997;3:917–21.
12. Altieri DC. The molecular basis and potential role of survivin in cancer diagnosis and therapy. Trends Mol Med 2001;7:542–7.
13. Li F, Ambrosini G, Chu EY, et al. Control of apoptosis and mitotic spindle checkpoint by survivin. Nature 1998;396:580–4.
14. Bao R, Connolly DC, Murphy M, et al. Activation of cancer-specific gene expression by the survivin promoter. J Natl Cancer Inst 2002;94:522–8.
15. Li F, Altieri DC. The cancer antiapoptosis mouse survivin gene: characterization of locus and transcriptional requirements of basal and cell cycle-dependent expression. Cancer Res 1999;59:3143–51.
16. Li F, Altieri DC. Transcriptional analysis of human survivin gene expression. Biochem J 1999;344 Pt 2:305–11.
17. Zwicker J, Lucibello FC, Wolfraim LA, et al. Cell cycle regulation of the cyclin A, cdc25C and cdc2 genes is based on a common mechanism of transcriptional repression. EMBO J 1995;14:4514–22.
18. Huang TG, Savontaus MJ, Shinozaki K, Sauter BV, Woo SL. Telomerase-dependent oncolytic adenovirus for cancer treatment. Gene Ther 2003;10:1241–7.
19. Wirth T, Zender L, Schulte B, et al. A telomerase-dependent conditionally replicating adenovirus for selective treatment of cancer. Cancer Res 2003;63: 3181–8.
20. Kim E, Kim JH, Shin HY, et al. Ad-mTERT-δ19, a conditional replication-competent adenovirus driven by the human telomerase promoter, selectively replicates in and elicits cytopathic effect in a cancer cell-specific manner. Hum Gene Ther 2003;14: 1415–28.
21. Takakura M, Kyo S, Kanaya T, et al. Cloning of human telomerase catalytic subunit (hTERT) gene promoter and identification of proximal core promoter sequences essential for transcriptional activation in immortalized and cancer cells. Cancer Res 1999;59:551–7.
22. Nagano S, Oshika H, Fujiwara H, Komiya S, Kosai K. An efficient construction of conditionally replicating adenoviruses that target tumor cells with multiple factors. Gene Ther. In press 2005.
23. Chen SH, Chen XH, Wang Y, et al. Combination gene therapy for liver metastasis of colon carcinoma *in vivo*. Proc Natl Acad Sci U S A 1995;92:2577–81.
24. Kawai T, Takahashi T, Esaki M, et al. Efficient cardiomyogenic differentiation of embryonic stem cell by fibroblast growth factor 2 and bone morphogenetic protein 2. Circ J 2004;68:691–702.
25. Yan P, Coindre JM, Benhattar J, Bosman FT, Guillou L. Telomerase activity and human telomerase reverse transcriptase mRNA expression in soft tissue tumors: correlation with grade, histology, and proliferative activity. Cancer Res 1999;59:3166–70.
26. Melton DW, Konecki DS, Brennand J, Caskey CT. Structure, expression, and mutation of the hypoxanthine phosphoribosyltransferase gene. Proc Natl Acad Sci U S A 1984;81:2147–51.
27. Terazaki Y, Yano S, Yuge K, et al. An optimal therapeutic expression level is crucial for suicide gene therapy for hepatic metastatic cancer in mice. Hepatology 2003;37:155–63.
28. Fukunaga M, Takamori S, Hayashi A, Shirouzu K, Kosai K. Adenoviral herpes simplex virus thymidine kinase gene therapy in an orthotopic lung cancer model. Ann Thorac Surg 2002;73:1740–6.
29. Nagano S, Yuge K, Fukunaga M, et al. Gene therapy eradicating distant disseminated micro-metastases by optimal cytokine expression in the primary lesion only: novel concepts for successful cytokine gene therapy. Int J Oncol 2004;24:549–58.
30. Bonnekoh B, Greenhalgh DA, Bundman DS, et al. Adenoviral-mediated herpes simplex virus-thymidine kinase gene transfer *in vivo* for treatment of experimental human melanoma. J Invest Dermatol 1996; 106:1163–8.
31. Kawakami Y, Li H, Lam JT, Krasnykh V, Curiel DT, Blackwell JL. Substitution of the adenovirus Serotype 5 Knob with a Serotype 3 Knob enhances multiple steps in virus replication. Cancer Res 2003;63: 1262–9.
32. Davydova J, Le LP, Gavrikova T, Wang M, Krasnykh V, Yamamoto M. Infectivity-enhanced cyclooxygenase-2-based conditionally replicative adenoviruses for esophageal adenocarcinoma treatment. Cancer Res 2004;64: 4319–27.
33. Liu Y, Ye T, Sun D, Maynard J, Deisseroth A. Conditionally replication-competent adenoviral vectors with enhanced infectivity for use in gene therapy of melanoma. Hum Gene Ther 2004;15:637–47.
34. Ito H, Kyo S, Kanaya T, Takakura M, Inoue M, Namiki M. Expression of human telomerase subunits and correlation with telomerase activity in urothelial cancer. Clin Cancer Res 1998;4:1603–8.

Gene Therapy (2005), 1–9

www.nature.com/gt

RESEARCH ARTICLE

An efficient construction of conditionally replicating adenoviruses that target tumor cells with multiple factors

S Nagano[1,2,3], H Oshika[4], H Fujiwara[5], S Komiya[2] and K Kosai[1,3,4]

[1]Division of Gene Therapy and Regenerative Medicine, Cognitive and Molecular Research Institute of Brain Diseases, Kurume University, Kurume, Japan; [2]Department of Orthopaedic Surgery, Graduate School of Medical and Dental Sciences, Kagoshima University, Kagoshima, Japan; [3]Department of Pediatrics and Child Health, Kurume University School of Medicine, Kurume, Japan; [4]Department of Gene Therapy and Regenerative Medicine, Gifu University School of Medicine, Gifu, Japan; and [5]Department of Cardiology, Respiratory and Nephrology, Regeneration & Advanced Medical Science, Graduate School of Medicine, Gifu University, Gifu, Japan

Despite the enormous potential of conditionally replicating adenoviruses (CRAs), the time-consuming and laborious methods required to construct CRAs have hampered both the development of CRAs that can specifically target tumors with multiple factors (m-CRA) and the efficient analysis of diverse candidate CRAs. Here, we present a novel method for efficiently constructing diverse m-CRAs. Elements involving viral replication, therapeutic genes, and adenoviral backbones were separately introduced into three plasmids of P1, P2, and P3, respectively, which comprised different antibiotic resistant genes, different ori, and a single loxP (H) sequence. Independently constructed plasmids were combined at 100% accuracy by transformation with originally prepared Cre and specific antibiotics in specific Escherichia coli; transfection of the resulting P1+2+3 plasmids into 293 cells efficiently generated m-CRAs. Moreover, the simultaneous generation of diverse m-CRAs was achieved at 100% accuracy by handling diverse types of P1+2 and P3. Alternatively, co-transfection of P1+3 and P2 plasmids into Cre-expressing 293 cells directly generated m-CRA with therapeutic genes. Thus, our three-plasmid system, which allows unrestricted construction and efficient fusion of individual elements, should expedite the process of generating, modifying, and testing diverse m-CRAs for the development of the ideal m-CRA for tumor therapy.
Gene Therapy advance online publication, 5 May 2005; doi:10.1038/sj.gt.3302540

Keywords: *conditionally replicating adenovirus; cancer; tumor-specific; Cre/lox recombination*

Introduction

One of the major obstacles to cancer gene therapy is inefficient and nonspecific gene delivery to cancer cells, leading to unsatisfactory outcomes in clinical trials due to recurrence from nontransduced tumor cells, even though some of the effective strategies, such as suicide gene therapy,[1,2] immunological gene therapy,[3,4] and their combinations[5] may treat nontransduced tumor cells to some degree and partially circumvent this problem. Conditionally replicating adenoviruses (CRAs), which selectively replicate in tumor cells, but not in normal cells, have the potential to circumvent this problem and to achieve tumor-specific gene delivery.[6,7] Moreover, CRA itself may be an attractive tool for innovative cancer therapy because selectively propagated adenovirus (Ad) induces the lysis of tumor cells. While various CRAs have been reported to date, the majority of them may be classified into two groups.[8] One is CRA that expresses E1 in a tumor-specific manner by the replacement of a native E1 promoter with various tumor-specific promoters.[9–12] The other is CRA with a partial deletion of the *E1* gene; the representatives are the mutant (mt) type of Ad lacking a p53-binding protein that is encoded by E1B55kD (ONYX-015),[13] and the mt Ad lacking an Rb-binding site of E1A (Δ24).[14,15] In the case of infection with the wild type of Ad, E1B55kD inhibits the p53-induced apoptosis of the host cell and enables Ad to continuously replicate in cells.[13,16] In addition, the interaction of adenoviral E1A with cellular Rb leads to the release of E2F transcription factor, which induces S-phase transition of the host cell in order to facilitate viral replication.[16] Based on these theories, neither mt ONYX-015 nor Δ24 may efficiently replicate in normal cells with intact Rb and p53, whereas both CRAs may actively replicate in the majority of tumor cells, disrupting the Rb-E2F pathway and/or p53 function.

However, a perfect CRA, which replicates efficiently in cancer cells but is completely attenuated in normal cells, has not yet been established in reality. Especially, the crucial problem of current CRAs is the insufficient or incomplete cancer specificity; that is, these CRAs do replicate in and cause some cytopathic effects, while greatly attenuated, in normal cells.[17–19] Recent studies suggested that CRAs with two or three tumor specific

Correspondence: Dr K Kosai, Division of Gene Therapy and Regenerative Medicine, Cognitive and Molecular Research Institute of Brain Diseases, Kurume University, 67 Asahi-machi, Kurume, Fukuoka, 830-0011, Japan
Received 2 November 2004; accepted 28 February 2005

factors enhanced their tumor specificity: mt E1A and mt E1B,[20] two tumor-specific promoters,[21] or a tumor-specific promoter and mt E1A.[12,22] In this regard, a promising approach to circumvent this obstacle might be combining and introducing multiple (more than three) tumor-specific factors into a single CRA. However, extensive and comparative studies on CRAs that are regulated with multiple tumor-specific factors (m-CRAs) are currently hampered by the lack of standardized methods to efficiently construct m-CRAs in contrast to well-established methods for efficiently constructing E1-deleted replication-incompetent Ad vectors.[23–25] It remains time-consuming and laborious to construct diverse m-CRAs using current methods; the requirement of additional modification steps hampers efficient production of diverse m-CRAs in large numbers by the same protocol. In addition, although functions of individual viral proteins have been largely elucidated,[16] the controversy over p53-dependent replication of the most representative CRA, ONYX-015,[13,17,18] suggests the necessity of extensive biological and systematic virological analyses of a large number of diverse m-CRAs in practice.

Here, we develop a novel method for the efficient construction of m-CRAs; this system simplifies and expedites the generation and modification of m-CRAs.

Results

Constitution of m-CRAs

One of the characteristic features of our method is the independent and unrestricted construction of three different regulatory elements in m-CRA, involving viral replication, therapeutic genes, and Ad backbones. To this end, these elements were separately introduced into three plasmids (Figure 1a). Replication-controllable plasmid P1 consists of wt or mt E1A and E1B sequences. Therapeutic gene-cloning plasmid P2 characteristically contains the tetracycline resistance gene (*tet*^{r}) and *R6Kγ ori*, which render this plasmid selectively amplified in only a specific type of *Escherichia coli* (*E. coli*) expressing the *pir* gene.[26] The Ad backbone plasmid P3 was described previously.[23] Potentially, more than seven tumor-specific factors can be introduced into the m-CRA (Figure 1a).

The use of different antibiotic resistance genes in all three plasmids, characteristically specific *ori* in P2 and unique I-*Ceu*I and PI-*Sce*I restriction sites in P1 and P3, enable the independent and unrestricted construction of three plasmids, and, subsequently, the feasible and rapid fusion of these three plasmids to generate a single CRA plasmid without using a regular ligation procedure. This is accomplished in the following manner (Figure 1b). Four variants of P1 vector with different combinations of wt or mt of E1A and E1B can be chosen at present. After the therapeutic gene and the promoters of interest were inserted into the multiple-cloning sites in P1 and P2, these two vectors were mixed and incubated with *Cre* aliquot. DH5α *E. coli* was transformed using all of the mixtures, and then grown on LB plates containing 5 μg/ml tetracycline. As P1 or P2 has either the kanamycin resistance gene (*kan*^{r}) or *R6Kγ ori* but not both, only the DH5α clone containing successfully recombined plasmid P1+2 will grow and form a colony on the LB plates containing tetracycline. P3 is digested with I-*Ceu*I and PI-*Sce*I, and ligated with I-*Ceu*I/PI-*Sce*I-digested P1+2, yielding a single P1+2+3 plasmid. Finally, this P1+2+3 plasmid, that is, Ad vector plasmid containing a replication-regulatory element and therapeutic gene, is linearized by *Pac*I, and transfected into 293 cells, as described previously.[5,23] Miniprep DNA can be used in all of the procedures, including the transfection; this feature increases the rapidity of this method and allows the handling of numerous samples simultaneously.

Preparation of Cre recombinase

Commercial *Cre* recombinase is so expensive that it prohibits the manipulation of a large number of samples in the present system. To circumvent this obstacle, we developed a feasible and inexpensive way to obtain a solution containing highly active *Cre* recombinase as follows. HepG2 cells, which demonstrated the highest level of transgene expression and the highest adenoviral gene transduction efficiency (data shown elsewhere), were infected with Ad.CA-Cre (Ad expressing Cre under the strongest CA promoter, which was kindly donated by I Saito) at an MOI of 30 for 2 days, and were then harvested and lysed in 200 μl buffer containing 20 mM Tris-HCl pH 7.5, 150 mM NaCl, 1 mM EDTA, and 10% glycerol by three rounds of freeze–thawing. The supernatants after centrifugation were collected and stored in aliquots at −80°C until use.

We compared the activity of our *Cre* aliquot with commercial products using two plasmids which had a single loxP sequence. At 1 day after the transformation of *E. coli* with our *Cre* aliquot and growth on 10 cm LB plates, several hundred colonies appeared and all colonies were correctly recombined to form a single plasmid (data not shown). Unexpectedly, two of the three commercial lots from two representative companies did not work well (no and one colony). Thus, the *Cre* activity in our aliquot was sufficiently high for reliable *Cre/lox* recombination in *E. coli*; we used this *Cre* aliquot for the following m-CRA construction (supernatant from one 10 cm dish allowed 200 samples of reaction).

Construction of CEA-responsive m-CRAs

To test the efficiency and the feasibility of this system, we generated carcinoembryonic antigen (CEA) responsive m-CRAs as an example, in which either wt or mt E1A was expressed under the transcriptional control of the CEA promoter (CEApr). Both types of m-CRA have mt E1B (E1BΔ55kD) downstream from the cytomegalovirus immediate-early gene enhancer/promoter (CMVpr). As a P2 plasmid, pUni/CMVpr-EGFP was used.

After the recombination of P1 and P2 with *Cre* aliquot, followed by the transformation of DH5α and growth, 10–50 colonies per 10 cm LB-tetracycline plate appeared. Notably, restriction enzyme analyses demonstrated that all of the clones contained the correctly recombined plasmid (pCEApr-E1A-CMVpr-E1BΔ55kD/CMVpr-EGFP or pCEApr-E1AΔ24–CMVpr-E1BΔ55kD/CMVpr-EGFP; we term each P1+2 plasmid as 'pP1-component/P2-component') (Figure 2a). The somewhat lower titer here than that shown in an earlier section was due to tetracycline selection, but not due to *Cre/lox* recombination efficiency, according to our preliminary studies (data not shown), whereas the result of 100% accuracy in 10–50

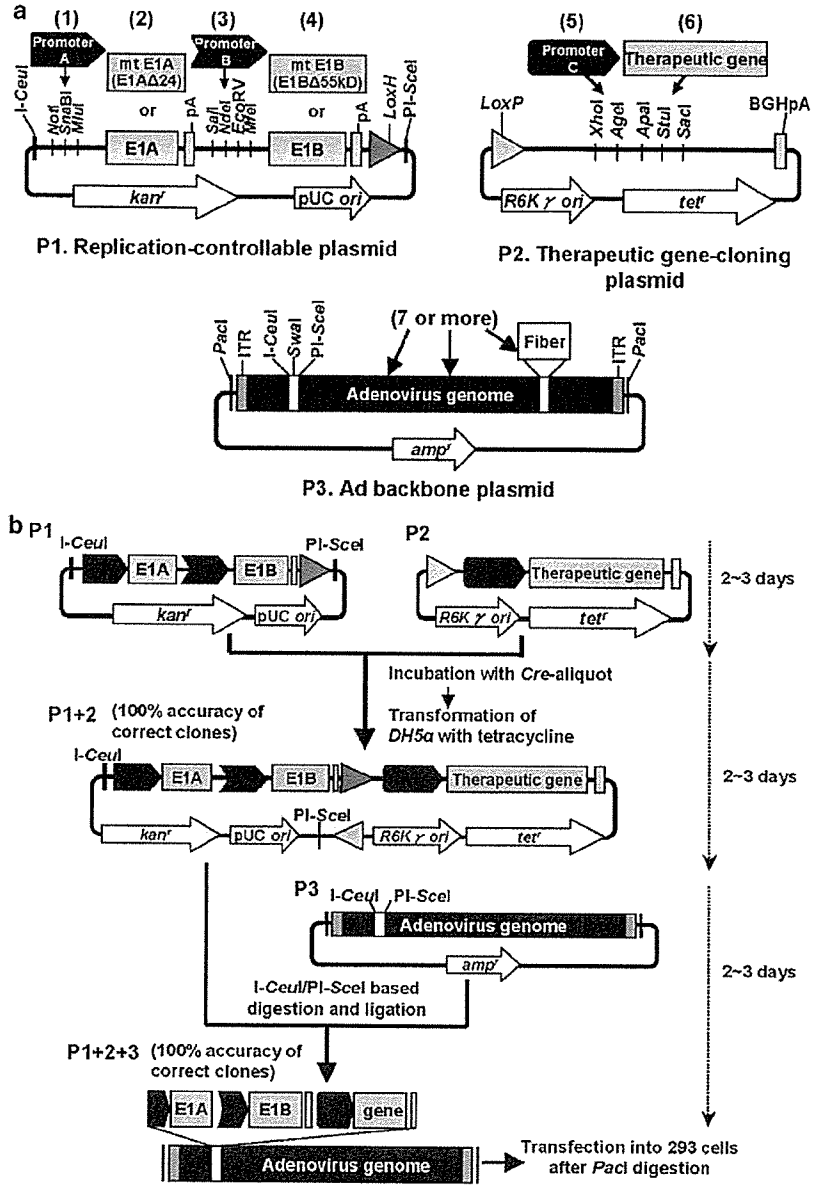

Figure 1 *The constitution and construction of m-CRA. (a) The constitution of the vector plasmids. Potentially, more than seven tumor-specific factors can be introduced into the m-CRA as follows. (1) Promoter A, which drives wt or mt E1A. (2) mt E1A, which lacks an Rb-binding site (E1AΔ24). (3) Promoter B, which drives wt or mt E1B. (4) mt E1B, which lacks a p53-binding protein that is encoded by E1B55kD (E1BΔ55kD). (5) Promoter C, which drives a therapeutic gene. (6) A therapeutic gene. (7 or more) Modification of Ad backbone, such as a fiber modification to modulate an infectivity. (b) The schematic representation of the m-CRA construction. All procedures, including the transfection into 293 cells, can be carried out using miniprep DNA.*

colonies was rather encouraging and sufficient for the present purpose.

Elements involving viral replication and the therapeutic gene were transferred from P1+2 to P3 (pAd.HM4) to generate P1+2+3 (pAd.HM4-CEApr-E1A-CMVpr-E1BΔ55kD/CMVpr-EGFP or pAd.HM4-CEApr-E1AΔ24–CMVpr-E1BΔ55kD/CMVpr-EGFP; we term each P1+2+3 adenoviral plasmid as 'pAd.P3-component-P1-component/P2-component'). The accuracy of such unique I-*Ceu*I/PI-*Sce*I-based ligation was almost 100% (Figure 2b), in accordance with the previous results.[23] Over 10 plaques appeared on 6 cm dishes 12 days after the transfection of *Pac*I-digested P1+2+3 into 293 cells. Notably, all of the plaques were EGFP-positive under fluorescent microscopy (Figure 2c). Accordingly, the PCR analyses of the DNA extracted from these m-CRAs verified that all of them were correct CEA-responsive m-CRA (CRA.CEApr-E1A-CMVpr-E1BΔ55kD/CMVpr-EGFP or CRA.CEApr-E1AΔ24-CMVpr-E1BΔ55kD/CMVpr-EGFP; we term each m-CRA as 'CRA.P1-component/P2-component') (Figure 2d).

Simultaneous construction of diverse types of m-CRAs

It would further facilitate extensive analyses of m-CRAs if numerous and diverse types of m-CRAs could be constructed at one time. To investigate this possibility, we first investigated whether initially constructed P1+3, that is, Ad backbone plasmid with a replication-regulatory

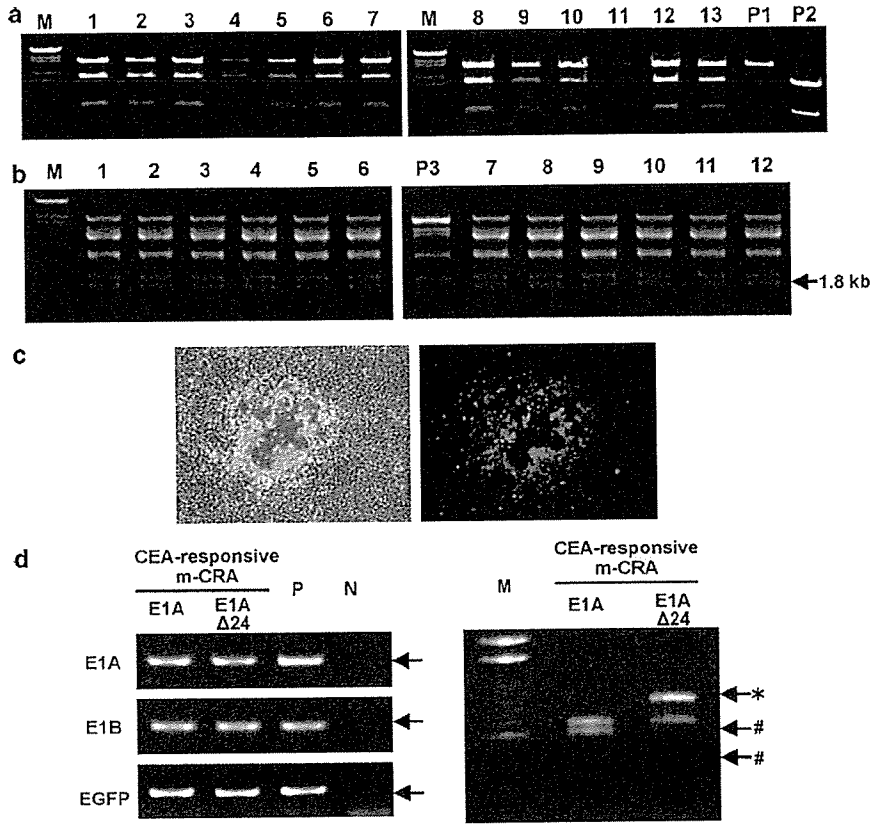

Figure 2 The efficiency and accuracy in the m-CRA construction on the protocol shown in Figure 1b. (a) Restriction enzyme analysis of P1+2 plasmid. After the reaction of pCEApr-E1A-CMVpr-E1BΔ55kD (P1) and pUni-CMVpr-EGFP (P2), 13 miniprep samples from E. coli colonies were digested by SalI and electrophoresed (M, marker. Lanes 1–13, each sample; P1, P1 plasmid; P2, P2 plasmid). The correct pattern (three bands consisting of P1-derived 6.3 kb band and P2-derived 3.2 and 1.2 kb bands) was seen in all samples, demonstrating 100% accuracy of correct clones containing P1+2 plasmid (pCEApr-E1A-CMVpr-E1BΔ55kD/CMVpr-EGFP) among all of the transformed clones. (b) Restriction enzyme analysis of P1+2+3 plasmid. After the reaction of P1+2 (pCEApr-E1A-CMVpr-E1BΔ55kD/CMVpr-EGFP) and P3 (pAd.HM4), 12 miniprep samples from E. coli colonies were digested with HindIII and electrophoresed (M, marker. Lanes 1–12, each sample; P3, P3 plasmid). The correct pattern was seen in all samples; the 1.8 kb band was indicative of the correct clone. (c) Phase-contrast (left) and fluorescent (right) microscopic pictures of one representative of m-CRA plaques (CRA.CEApr-E1A-CMVpr-E1BΔ55kD/CMVpr-EGFP) on 293 cells 10 days after transfection of PacI-digested pAd.HM4-CEApr-E1A-CMVpr-E1BΔ55kD/CMVpr-EGFP. (d) PCR analyses of genomic DNA extracted from m-CRA plaques. PCR was performed with three different primer sets of S-E1A-1/AS-E1A-1, S-E1B-1/AS-E1B-1, and S-EGFP/AS-EGFP to detect E1A, E1A, and EGFP DNA, respectively, in CEA-responsive m-CRAs (E1A; CRA.CEApr-E1A-CMVpr-E1BΔ55KD/CMVpr-EGFP, and E1AΔ24; CRA.CEApr-E1AΔ24-CMVpr-E1BΔ55kD/CMVpr-EGFP) (the left picture). P, positive control plasmid DNA corresponding to each of primer sets. N, nontemplate DNA. To distinguish these two CEA-responsive m-CRAs, PCR products amplified with the primer sets of S-HM5 and AS-E1A-1 were digested with BstXI, of which recognition sites existed in the Rb-binding domain of E1A and Ad backbone (the right picture). The correct pattern was seen in all samples of both types of m-CRA; the 0.8 kb band (*), and the 0.5 and 0.3 kb bands (#) were indicative of m-CRA with mt E1A (E1AΔ24), and that with wtE1A, respectively.

element, might be recombined with therapeutic gene-cloning vector P2 in the same way as the recombination of P1 and P2 (Figure 3a). P1+3 (pAd.HM4-CEApr-E1A-CMVpr-E1BΔ55kD) was constructed by transferring replication-regulatory elements from P1 (pCEApr-E1A-CMVpr-E1BΔ55kD) to P3 (pAd.HM4) with I-*Ceu*I/PI-*Sce*I-based ligation. After incubating P1+3 (pAd.HM4-CEApr-E1A-CMVpr-E1BΔ55kD) and P2 (pUni/CMVpr-EGFP) with *Cre* aliquot, DH5α was transformed with all of the mixtures and grew on LB plates with tetracycline. After 1 day, about 30 colonies appeared on a 10 cm dish, and all of them contained correctly recombined P1+2+3 plasmid (pAd.HM4-CEApr-E1A-CMVpr-E1BΔ55kD/CMVpr-EGFP) (Figure 3b). Thus, both the efficiency and accuracy of the recombination/transformation of P1+2 and P3 were similarly high in comparison with those of P1 and P2, as shown in the earlier section, although P1+3 was a much larger plasmid than P1 alone.

Next, the feasibility of simultaneously constructing several different types of m-CRAs was tested. DH5α *E. coli* in each of 10 tubes containing the same P2 (pUni/CMVpr-EGFP) and *Cre* aliquot was transformed by each of 10 different types of P1+3 plasmid. At 1 day after the growth on LB-tetracycline plates, 3–52 colonies appeared on each of the 10 cm plates, and all colonies were correctly recombined plasmids (Figure 3c).

Furthermore, we examined whether more different tumor-specific factors including therapeutic genes can be correctly inserted into m-CRAs with the present system. Eight different m-CRAs that contain six tumor-specific factors, that is, (1) human telomerase reverse transcriptase promoter (TERTpr) driving E1A, (2) wt or mt E1A, (3) human E2F promoter (E2Fpr) driving E1B, (4) mt E1B,

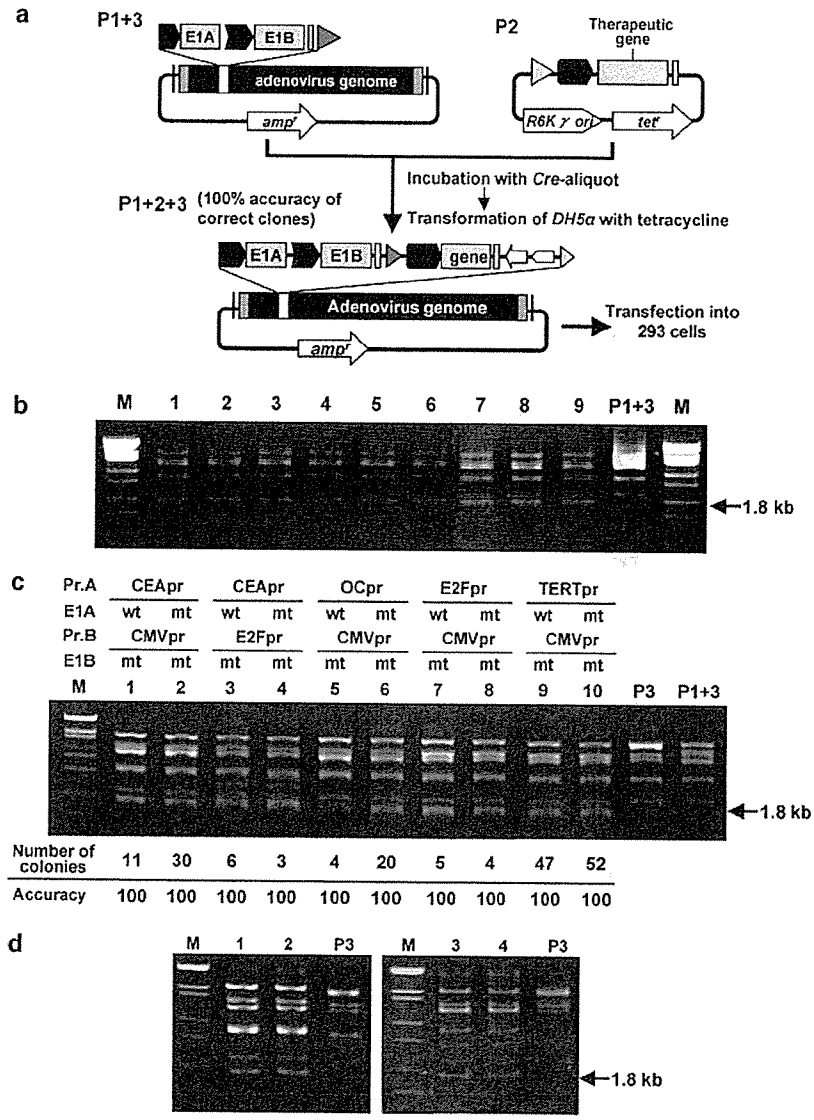

Figure 3 Simultaneous construction of diverse types of m-CRA plasmids. (a) The schematic representation. Initially constructed P1+3, that is, Ad backbone plasmid with a replication-regulatory element, can be recombined with therapeutic gene-cloning vector P2 to yield a single P1+2+3 plasmid. (b) Restriction enzyme analysis of genomic DNA extracted from clones transformed with P1+3 (pAd.HM4-CEApr-E1A-CMVpr-E1BΔ55kD) and P2 (pUni/CMVpr-EGFP). HindIII digestion of miniprep samples demonstrated the correct pattern of P1+2+3 plasmid (pAd.HM4-CEApr-E1A-CMVpr-E1BΔ55kD/CMVpr-EGFP) in all of the transformed clones (M, marker. Lanes 1–9, each sample; P1+3, P1+3 plasmid); the 1.8 kb band was indicative of the correct clone. (c, d) Simultaneous construction of several different types of m-CRAs with this protocol. (c) DH5α E. coli in each of 10 tubes containing the same P2 (pUni/CMVpr-EGFP) and each of 10 different types of P1+3 plasmid, which were preincubated with the Cre aliquot, were transformed and grew with tetracycline. HindIII-digestion analysis was carried out in the same manner as above, and one representative picture per group was shown here. Numbers of colonies per 10 cm plate appeared and the accuracy (the percentage of the correct clones; clones in each group were carefully analyzed with several different types of restriction enzymes although data were not shown here) in each group is shown below the picture (M, marker. Lanes 1–10, each sample; Pr.A, promoter driving wt or mt E1A; Pr.B, promoter driving wt or mt E1B; P3, P3 plasmid; P1+3, P1+3 plasmid). The 1.8 kb band was indicative of the correct clone. (d) Four different CRAs which contain six tumor-specific factors were constructed and the P1+2+3 plasmids were analyzed by HindIII digestion (M, marker. Lane 1, pAd.HM4-TERTpr-E1A-E2Fpr-E1BΔ55kD/Surv.pr-p53; Lane 2, pAd.HM4-TERTpr-E1AΔ24-E2Fpr-E1BΔ55kD/Surv.pr-p53; Lane 3, pAd.HM12-TERTpr-E1A-E2Fpr-E1BΔ55kD/Surv.pr-tk; each sample; Lane 4, pAd.HM12-TERTpr-E1AΔ24-E2Fpr-E1BΔ55kD/Surv.pr-tk; P3, P3 plasmid).

(5) mouse survivin promoter (Surv.pr) or CMVpr driving therapeutic gene, and (6) therapeutic gene (p53 or herpes simplex virus thymidine kinase (HSV-tk), were successfully constructed (Figure 3d and data not shown).

Thus, it was shown that simultaneous construction of diverse m-CRAs was, in fact, feasible using the present system.

Therapeutic gene insertion into m-CRA directly in Cre-expressing 293 cells (alternative protocol)

We further hypothesized that two types of plasmids, P1+3 and P2, might be recombined directly in *Cre*-expressing 293 cells (Figure 4a). To assess this possibility, P1+3 (pAd.HM4-CEApr-E1A-CMVpr-E1BΔ55kD) and